Biosynthesis system of Synechan, a sulfated exopolysaccharide, in the model cyanobacterium *Synechocystis* sp. PCC 6803

Kaisei Maeda[1,2], Yukiko Okuda[1], Gen Enomoto[1], Satoru Watanabe[2], Masahiko Ikeuchi[1,3]

[1]Department of Life Sciences (Biology), Graduate School of Arts and Sciences, University of Tokyo, Komaba, Meguro, Tokyo 153-8902, Japan

[2](present address) Department of Bioscience, Tokyo University of Agriculture, Sakuragaoka, Setagaya-ku, Tokyo 156-8502, Japan

[3]Faculty of Education and Integrated Arts and Sciences, Waseda University, Tokyo 162-8480, Japan

Abstract

Extracellular polysaccharides of bacteria contribute to biofilm formation, stress tolerance, and infectivity. Cyanobacteria, the oxygenic photoautotrophic bacteria, uniquely and widely have sulfated extracellular polysaccharides and they may utilize the polysaccharides for survival in nature. In addition, sulfated polysaccharides of cyanobacteria and other organisms have been focused as beneficial biomaterial. However, very little is known about their biosynthesis machinery and function in cyanobacteria. Here we found that the model cyanobacterium, *Synechocystis* sp. PCC 6803, formed bloom-like cell aggregates using sulfated extracellular polysaccharides (designated as synechan) and identified whole set of genes responsible for synechan biosynthesis and its transcriptional regulation, thereby suggesting a model for the synechan biosynthesis apparatus. Because similar genes are found in many cyanobacterial genomes with wide variation, our findings may lead elucidation of various sulfated polysaccharides, their functions, and their potential application in biotechnology.

Introduction

Bacterial extracellular polysaccharides establish biofilms for nutrient supply and stress avoidance, and they sometimes support cellular activities such as motility and infectivity (*Woodward and Naismith, 2016*). Generally, the polysaccharide chains consist of a few types of sugars (with or without chemical modifications) and are anchored on cells (capsular polysaccharides, CPS) or exist as nonanchored exopolysaccharides (EPS). Nonetheless, their molecular structures vary greatly, e.g., branching schemes, sugar constituents, and modifications, and thus their physical properties also vary. Bacterial extracellular polysaccharides and lipopolysaccharides are produced and exported via three distinct pathways: the Wzx/Wzy-dependent pathway, ABC-dependent pathway, and synthase-dependent pathway (*Schmid et al., 2015*). Every bacterium can produce several extracellular polysaccharides, and production often depends on environmental conditions. Some extracellular polysaccharides have been appropriated for use as biopolymers for food, cosmetics, medicine (*Freitas et al., 2014, Lapasin and Pricl, 1995*).

Cyanobacteria, the oxygenic photoautotrophic bacteria that inhabit almost every ecosystem on Earth, contribute to the global photosynthetic production (*Flombaum et al., 2013, Mangan et al., 2016*). Cyanobacteria produce various extracellular polysaccharides to form colonies, which are planktonic or attached on solid surfaces, likely to stay in a phototrophic niche in nature (*De Philippis and Vincenzini, 1998*). A notable example is the water bloom, a dense population of cyanobacterial cells that floats on the water surface and often produces cyanotoxins and extracellular polysaccharides (*Huisman et al., 2018*). The extracellular polysaccharides are also important for photosynthetic production of cyanobacteria and their application (*Kumar et al., 2018*). However, very little is known about their biosynthesis except for extracellular cellulose. A thermophilic cyanobacterium (*Thermosynechococcus vulcanus*) accumulates cellulose to form cell aggregation (*Kawano et al., 2011*). This cellulose is produced by cellulose synthase with unique tripartite system and regulations (*Enomoto et al., 2015, Maeda et al., 2018*). In the cyanobacterial genomes, there are still many putative genes for extracellular polysaccharide biosynthesis.

49 Uniquely, many cyanobacterial extracellular polysaccharides are sulfated, i.e., as a sugar
50 modification (*Pereira et al., 2009*). Sulfated polysaccharides are also produced by animals (as
51 glycosaminoglycan in the extracellular matrix such as heparan sulfate) and algae (as cell-wall
52 components such as carrageenan) but are scarcely known in other bacteria or plants (*Ghosh et al., 2009*).
53 Major examples of cyanobacterial sulfated polysaccharides are spirulan from *Arthrospira platensis*
54 (vernacular name, "Spirulina"), sacran from *Aphanothece sacrum* (vernacular name, "Suizenji-Nori")
55 and cyanoflan from *Cyanothece* sp. CCY 0110 (*Mota et al., 2020, Mouhim et al., 1993, Okajima et al.,*
56 *2008*). These sulfated polysaccharides are used for formation of colony and biofilm and may be
57 functionally relevant to the ecology of cyanobacteria (*Fujishiro et al., 2004*). In addition, the
58 bioactivities (antiviral, antitumor, and anti-inflammatory) of sulfated polysaccharides from
59 cyanobacteria were reported, too (*Flores et al., 2019a, Hayashi et al., 1996, Ngatu et al., 2012*).
60 However, very little is known about their biosynthesis machinery and physiological functions. On the
61 other hand, biosynthesis and modification of animal sulfated polysaccharides have been extensively

62 studied because of their importance to tissue protection, tissue development, and immunity (*Karamanos*

63 *et al., 2018, Sasisekharan et al., 2006*) and potential applications in healthy foods, biomaterials, and

64 medicines (*Jiao et al., 2011, Wardrop and Keeling, 2008*).

65 The poor understanding about cyanobacterial sulfated polysaccharide biosynthesis is probably

66 due to low or no accumulation of sulfated polysaccharides in typical model species (*Pereira et al., 2009*).

67 More than three decades ago, Panoff et al. reported sulfated polysaccharides in two related model

68 cyanobacteria, *Synechocystis* sp. PCC 6803 and *Synechocystis* sp. PCC 6714 (hereafter *Synechocystis*

69 6803 and *Synechocystis* 6714) (*Panoff et al., 1988*). Recently, Flores et al. confirmed sulfated

70 polysaccharides and reported their enhanced accumulation in a sigma factor *sigF* mutant for global cell

71 surface regulation in *Synechocystis* 6803 (*Flores et al., 2019b*). In parallel, several papers have studied

72 genes that could be involved in extracellular polysaccharides biosynthesis in *Synechocystis* 6803, but no

73 clear results were obtained about the sulfated polysaccharide (*Fisher et al., 2013, Foster et al., 2009,*

74 *Jittawuttipoka et al., 2013, Pereira et al., 2019*). Here we found that a motile substrain of *Synechocystis*

6803 showed bloom-like cell aggregation and sulfated EPS production, but a non-motile substrain (a standard substrain for photosynthesis study) did not. By gene disruption and overexpression, we first identified a whole set of genes responsible for sulfated EPS biosynthesis and its regulatory system, opening the way to engineering of their production.

Results

Bloom formation and EPS accumulation in Synechocystis *sp. PCC 6803*

We fortuitously found that a motile substrain of *Synechocystis* 6803 produces EPS and forms floating cell aggregates resembling a typical cyanobacterial bloom. We established a two-step culture regime (2-day bubbling culture and subsequent standing culture without bubbling under continuous light) for reproducible formation of bloom-like aggregates (Fig. 1A, B). The first (bubbling) step allows for cell propagation and EPS production, whereas the second (standing) step allows for heavy-cell aggregation and flotation, even though *Synechocystis* 6803 does not possess genes for intracellular gas

vesicles (*Harke et al., 2016*). In *Synechocystis* 6803, cell flotation accompanying the generation of extracellular gas bubbles was suppressed by inactivation of photosynthesis (Fig. 1C), suggesting that gas derived from photosynthesis drives the upward movement of cells embedded in viscous EPS. The non-motile, glucose-tolerant substrain—commonly used for photosynthesis research—did not aggregate or float.

We first isolated crude EPS from the bloomed culture by membrane filtration (Fig. S1A). The crude EPS consisted of polysaccharide but very little protein or nucleic acid, and its abundance remained unchanged during the second culture step (Fig. S1B). As a common feature of diverse EPS biosynthesis systems in bacteria, membrane-bound glycosyltransferases are particularly important (*Schmid et al., 2015*). So, we screened such glycosyltransferase genes by disruption and revealed that *slr5054* is essential for bloom formation (Fig. 1D, E and Fig. S2). The EPS preparation was improved by removing cells before filtration to avoid cell-associated polysaccharides such as CPS (Fig. 1F). Δ*slr5054* lacked most of the EPS present in the wild type (WT), whereas the CPS and free polysaccharide fractions were

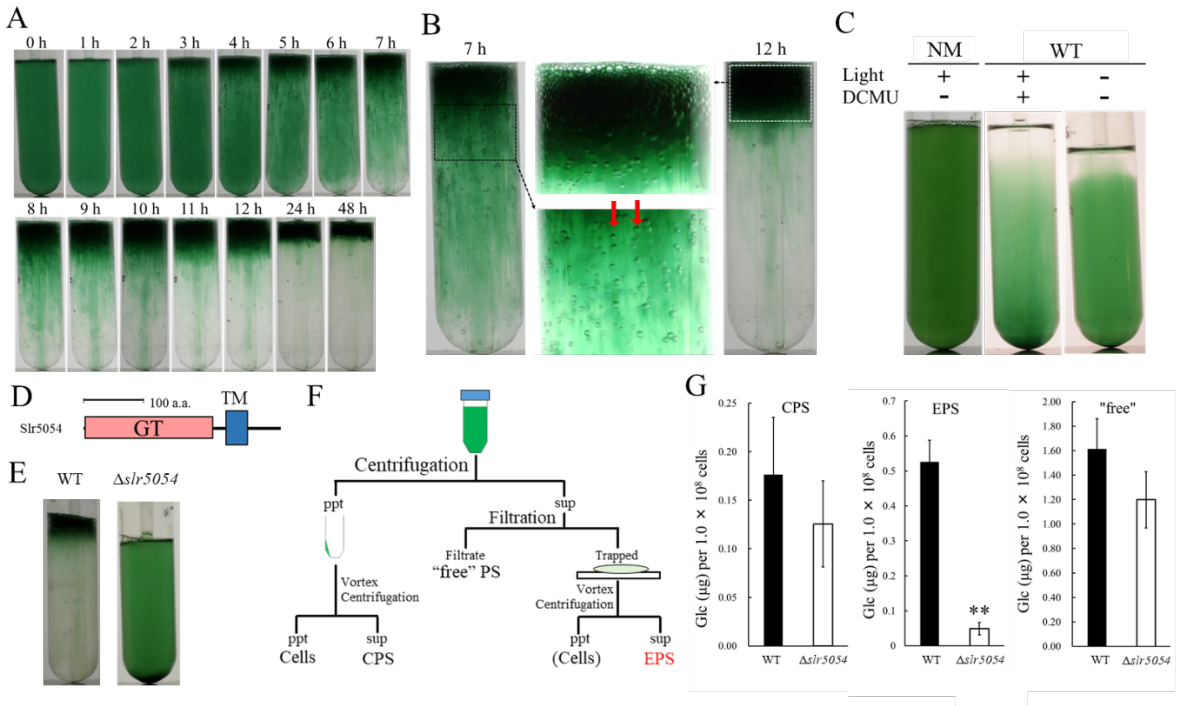

Figure 1 Bloom formation and EPS isolation.

A, Time course of bloom formation by WT *Synechocystis* 6803 during the second step of culture. Extracellular gas bubbles are formed and trapped in viscous EPS (~1 h). Green vertical columns with bubbles become apparent at 4 h. Those trapped gas bubbles slowly rise together with the viscous columns. **B**, Enlarged images showing gas bubbles trapped in EPS. Vertically aligned bubbles are indicated by red arrows. **C**, Lack of bloom formation in the non-motile substrain (NM) or WT with or without light and the photosynthesis inhibitor DCMU at 48 h of the second step of culture. **D**, Domain architecture of Slr5054. GT, glycosyltransferase domain; TM, transmembrane region. **E**, Lack of bloom formation in Δ*slr5054* after standing culture for 48 h. **F**, Isolation of EPS from the first step of culture. Cells and CPS were removed from the culture by centrifugation, and EPS in the supernatant was separated from "free" polysaccharide (PS) by membrane filtration followed by a second centrifugation to remove residual cells. CPS was collected from the cell pellet after vortexing and centrifugation. **G**, Sugar content of fractions from WT and Δ*slr5054*. Error bars represent SD (n = 3, $^{**}P < 0.005$).

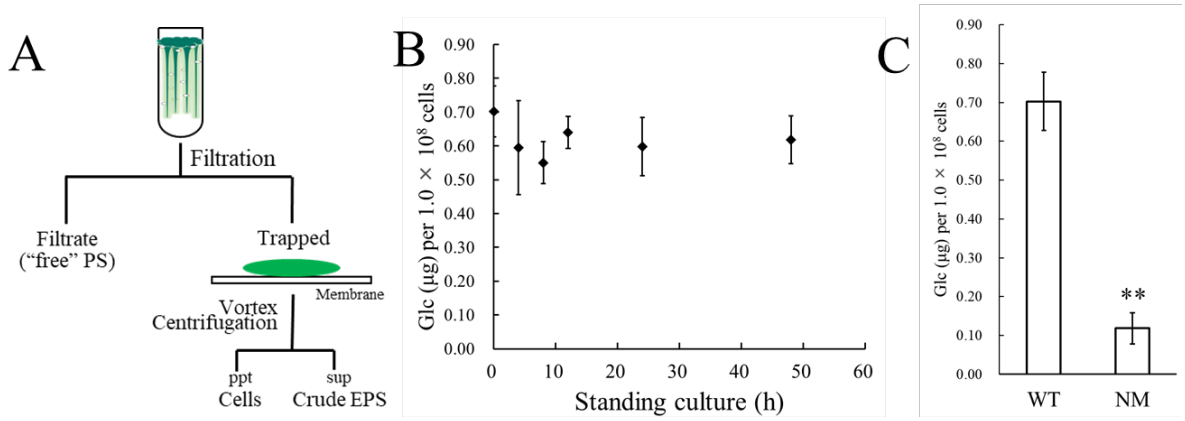

Figure S1. Isolation of crude EPS and sugar analysis.

A, Protocol for isolating crude EPS from the bloomed culture. The bloom, including EPS and cells at the end of the second (standing) step of culture, was trapped by membrane filtration, and crude EPS was recovered from the bloom by vortexing and centrifugation. PS, polysaccharide; ppt, precipitate; sup, supernatant. **B,** Time course of sugar accumulation in the crude EPS during the standing culture. **C,** Sugar content of the crude EPS from WT, and a non-motile glucose-tolerant substrain (NM). Error bars represent SD (n = 3, $^{**}P < 0.005$).

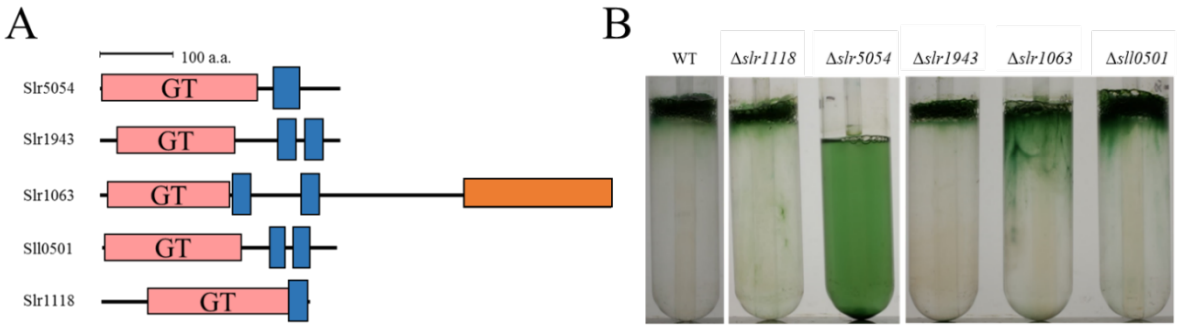

Figure S2. Bloom formation by several glycosyltransferase mutants.

A, Domain architecture of membrane-bound glycosyltransferases. Red box, glycosyltransferase domain (GT); blue box, transmembrane region; orange box, glycogen phosphorylase domain. **B,** Bloom formation by mutants after the second step of culture.

similar in the WT and Δ*slr5054* (Fig. 1G). Then we performed Alcian blue staining to examine the acidity of the EPS (Fig. S3). Generally, sulfated polysaccharides are stained at pH 0.5 condition, while acidic polysaccharides, which contain sulfate groups and/or carboxylate groups (such as uronic acids and carboxylate modification) are stained at pH 2.5 condition (*Bellezza et al., 2006*). The EPS from WT was clearly stained under both pH conditions, strongly suggestive of the sulfate modification.

Gene cluster for the biosynthesis of viscous polysaccharides

slr5054 resides on a megaplasmid, pSYSM, in a large gene cluster (*sll5042–60*), which we named *xss* (extracellular sulfated polysaccharide biosynthesis) (Fig. 2A, *xssA–xssS*). This cluster includes two genes for sulfotransferases (*xssA*, *xssE*), eight genes for glycosyltransferases (*xssB*, *xssC*, *xssG*, *xssI*, *xssM*, *xssN*, *xssO*, *xssP*), three genes for the polysaccharide polymerization system (Wzx/flippase; *xssH*, Wzy/polymerase; *xssF*, and polysaccharide co-polymerase [PCP]; *xssK*), one gene for a putative transcriptional regulator (*xssQ*), a pair of genes for the bacterial two-component

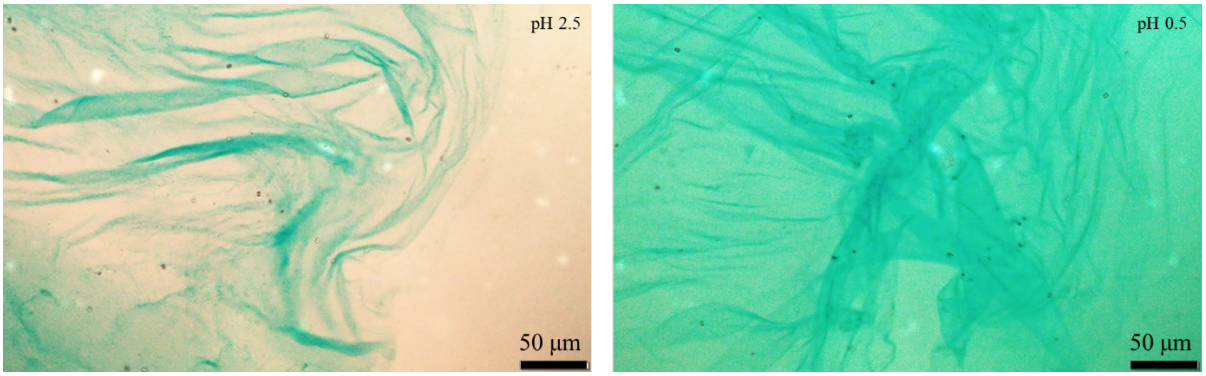

Figure S3 Alcian blue staining of EPS from WT.

The microscopy images of isolated EPS from WT culture (Fig. 1g) stained with alcian blue at pH 2.5 (left) and pH 0.5 (right).

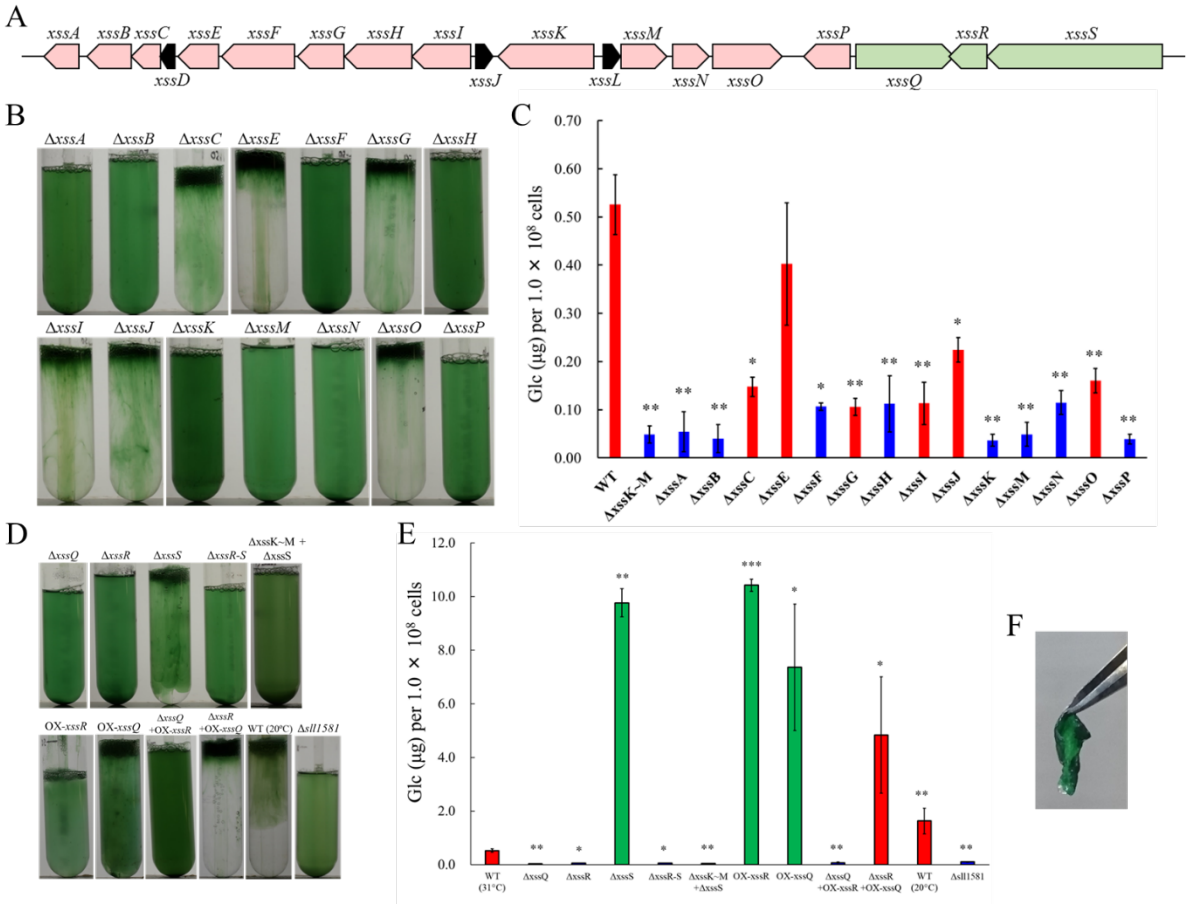

Figure 2 The *xss* gene cluster and phenotype of *xss* mutants.

A, The *xss* gene cluster. Red, polysaccharide biosynthesis genes; green, regulatory genes; black, genes of unknown function. **B,** Bloom formation by the mutants carrying disruptions in the polysaccharide biosynthesis *xss* genes. **C**, Total sugar content (μg glucose per 1×10^8 cells) of the EPS fraction from mutants in b. Red bars, bloom-forming mutants; blue bars, non-bloom-forming mutants. Error bars represent SD (WT grown at 20°C, n = 6; others, n = 3). Statistical significance was determined using Welch's *t* test (*$P < 0.05$, **$P < 0.005$, ***$P < 0.0005$). **D,** Bloom formation by regulatory mutants, WT grown at 20ºC, and OPX mutant (Δ*sll1581*). **E,** Total sugar content of the EPS fraction from mutants in d. Red bars, bloom-forming mutants; green bars, excess-bloom-forming mutants. **F,** A sheet of OX-*xssR* cells was stripped off from the agar plate by tweezers. The culture temperature was 31°C unless otherwise stated.

160 phosphorelay system (*xssR*, *xssS*), and genes encoding several small proteins of unknown function

161 (Table S1, Fig. 2A). All genes except those of unknown function were disrupted individually with a

162 read-through cassette, and segregation was confirmed by colony PCR (Fig. S4). Bloom formation and

163 sugar content of the EPS fraction were reduced in many mutants (Fig. 2B, C). In particular, bloom

164 formation was completely abolished in Δ*xssA*, Δ*xssB*, Δ*xssF*, Δ*xssH*, Δ*xssK*, Δ*xssM*, Δ*xssN*, and Δ*xssP*,

165 in which EPS accumulation was also suppressed. Certain glycosyltransferase mutants (Δ*xssC*, Δ*xssG*,

166 Δ*xssI*, Δ*xssO*) formed blooms but accumulated little EPS, and neither bloom formation nor EPS

167 accumulation was substantially altered in one sulfotransferase mutant (Δ*xssE*). In general, the Wzx/Wzy

168 system in bacteria produces various EPS, lipopolysaccharides, and CPS through four steps: (i)

169 biosynthesis of a heterooligosaccharide repeat unit on a lipid linker at the cytoplasmic side of the plasma

170 membrane by a series of glycosyltransferases and modification enzymes, (ii) flip-out of the unit to the

171 periplasmic side by Wzx, (iii) polymerization by transfer of the nascent polysaccharide chain to the

172 repeat unit by Wzy, and (iv) export of the EPS chain through the periplasm and outer membrane via PCP

173 **Table S1.** Summary of *Synechocystis* 6803 Xss proteins.

Category	Name	Locus tag	Function	Importance	Regulation
Polysaccharide chain biosynthesis	XssP	*sll5057*	Priming GT	+++	+
	XssB	*sll5043*	GT	+++	+
	XssM	*slr5054*	GT	++	−
	XssN	*slr5055*	GT	++	+
	XssC	*sll5044*	GT	+	+
	XssG	*sll5048*	GT	+	−
	XssI	*sll5050*	GT	+	−
	XssO	*slr5056*	GT	+	+
Modification	XssA	*sll5043*	ST	+++	+
	XssE	*sll5046*	ST	±	+
Translocation	XssH	*sll5049*	Wzx/Flippase	++	−
Polymerization and exportation	XssF	*sll5047*	Wzy/Polymerase	++	−
	XssK	*sll5052*	PCP-2a/Exporter	+++	−
	XssT	*sll1581*	OPX/Exporter	++	−
Regulation	XssQ	*slr5058*	Transcriptional regulator	+++	n.d.
	XssR	*sll5059*	Response regulator	+++	n.d.
	XssS	*sll5060*	Sensor histidine kinase	+++	n.d.

174

175 Function: GT, glycosyltransferase; ST, sulfotransferase; PCP, polysaccharide co-polymerase; OPX,

176 outer-membrane polysaccharide export protein.

177 Importance: contribution in EPS accumulation.

178 Regulation: transcriptional regulation of *xss* genes by XssQ/R/S. n.d., not determined.

179

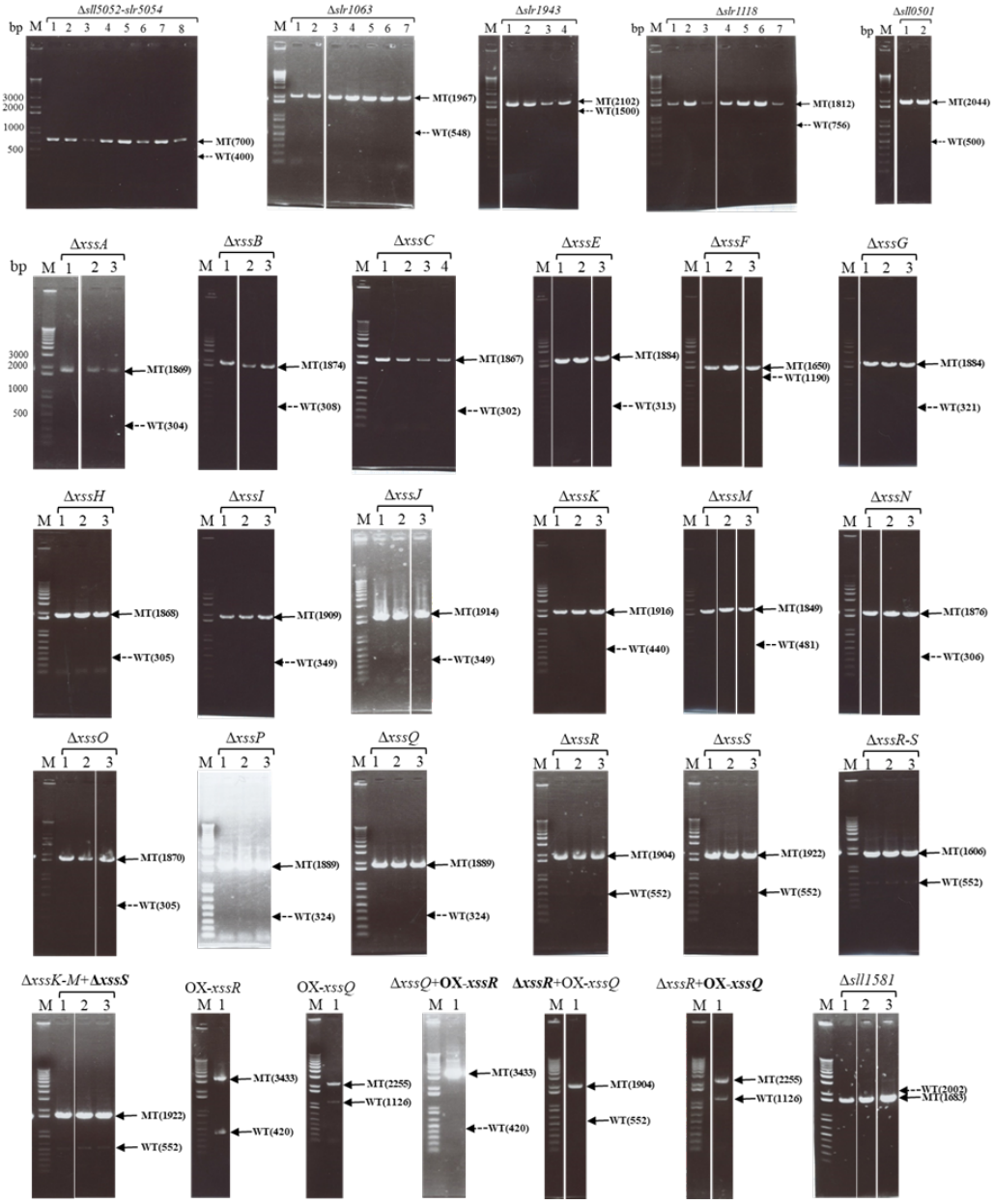

Figure S4. Agarose gel electrophoresis to assess segregation of mutants based on PCR data. M indicates marker lane, and the numbers above each lane indicate the different clones. The band positions of wild type (WT) and mutants (MT) are shown at the right, with theoretical lengths in nt. A solid arrow indicates the existence of the band; a dotted arrow indicates the absence of the band. The bold text in the strain names indicates the region assessed by PCR.

187 and the outer-membrane polysaccharide export protein (OPX) (*Islam and Lam, 2014, Schmid et al.,*

188 *2015*). It is very likely that the *xss* cluster harbors a whole set of genes for the Wzx/Wzy-dependent

189 pathway except a gene for OPX.

190

191 ***Regulation of the sulfated EPS biosynthesis***

192 The sensory histidine kinase mutant Δ*xssS* accumulated a much larger amount of EPS than

193 WT, whereas mutants of the cognate response regulator *xssR* and transcriptional regulator *xssQ* had a

194 null phenotype with regard to both bloom formation and EPS accumulation (Fig. 2D, E, Table S2). The

195 double mutant Δ*xssS*/Δ*xssR* had a phenotype similar to that of Δ*xssR*. Overexpression of *xssR* or *xssQ*

196 (OX-*xssR*, OX-*xssQ*) resulted in strong bloom formation as well as marked accumulation of viscous

197 EPS, similar to that seen for Δ*xssS*. The combination of *xssQ* disruption and *xssR* overexpression

198 (Δ*xssQ*+OX-*xssR*) abrogated bloom formation and EPS accumulation, whereas the combination of *xssQ*

199 overexpression and *xssR* disruption (Δ*xssR*+OX-*xssQ*) resulted in a pronounced phenotype of bloom

200 formation and EPS accumulation. These results suggested that the sensor histidine kinase XssS
201 suppresses the response regulator XssR, leading to activation of the transcriptional activator XssQ.
202 Notably, the OX-*xssR* and OX-*xssQ* strains formed sticky, non-motile, biofilm-like colonies on agar
203 plates that could be picked by tweezers (Fig. 2F).

204 XssQ is a new type of the signal transduction ATPase with numerous domains (STAND)
205 protein, because it harbors an N-terminal helix-turn-helix transcriptional DNA-binding domain (Fig.
206 S5). Typical STAND proteins possess a three-domain module with ATPase activity and are involved in
207 processes such as apoptosis and immunity in animals, plants, and some bacteria (*Danot et al., 2009*).
208 Using real-time quantitative PCR (qPCR), we compared gene expression in the *xss* cluster for WT, Δ*xssS*,
209 and Δ*xssQ* (Fig. 3A). Expression of five genes (*xssA*, *xssB*, *xssE*, *xssN*, *xssP*) was very low in Δ*xssQ*
210 compared with WT, whereas that of *xssF*, *xssH*, and *xssK* was not substantially affected. These results
211 suggested that XssQ transcriptionally activates genes encoding sulfotransferases and certain
212 glycosyltransferases but not genes for polymerization and export via the Wzx/Wzy system. qPCR

213 **Table S2.** EPS accumulation and bloom formation by WT *Synechocystis* 6803 and *xss* mutants.

Strain name	Classification	Glc (μg) per 1.0 × 10^8 cells	Ratio (% WT)	Bloom
WT(31°C)		0.526 ± 0.062	100.0	+
WT(20°C)		1.629 ± 0.472	309.9	+
Δ*xssA*	ST3	0.054 ± 0.042	10.4	-
Δ*xssB*	GT2	0.040 ± 0.029	7.7	-
Δ*xssC*	GT25	0.148 ± 0.020	28.1	+
Δ*xssE*	ST3	0.402 ± 0.127	76.6*	+
Δ*xssF*	Wzy / polymerase	0.107 ± 0.008	20.3	-
Δ*xssG*	GT4	0.105 ± 0.018	20.1	+
Δ*xssH*	Wzx / Flippase	0.112 ± 0.059	23.0	-
Δ*xssI*	GT4	0.113 ± 0.044	21.6	+
Δ*xssJ*	-	0.224 ± 0.025	42.6	+
Δ*xssK*	PCP2a	0.037 ± 0.012	7.0	-
Δ*xssM*	GT2	0.049 ± 0.025	14.6	-
Δ*xssN*	GT26	0.115 ± 0.025	21.8	-
Δ*xssO*	GT2	0.161 ± 0.025	30.6	+
Δ*xssP*	Priming GT	0.039 ± 0.010	7.4	-
Δ*xssQ*	Transcriptional regulator	0.036± 0.010	6.8	-
Δ*xssR*	Response regulator	0.059 ± 0.009	11.2	-
Δ*xssS*	Histidine kinase	9.770 ± 0.524	1860	++
Δ*xssR-S*		0.062 ± 0.008	11.8	-
Δ*xssK~M*+Δ*xssS*		0.044 ± 0.013	8.4	-
OX-*xssR*		10.426 ± 0.225	1984	++
OX-*xssQ*		7.359 ± 2.36	1400	++
Δ*xssQ*+OX-*xssR*		0.077 ± 0.027	14.6	-
Δ*xssR*+OX-*xssQ*		4.837 ± 2.169	920	+
Δ*sll1581* (*xssT*)	OPX / exporter	0.103 ± 0.012	19.6	-

214

215 Classification: ST, sulfotransferase; GT, glycosyltransferase; PCP, polysaccharide co-polymerase; OPX,
216 outer-membrane polysaccharide export protein. Total sugar content of the EPS fraction is expressed as
217 μg glucose / 1 × 10^8 cells. The errors are based on SD (n = 3). *Close to the detection limit. EPS
218 accumulation ratio, percent of WT grown at 31°C. Bloom formation is summarized from Fig. 2.

219

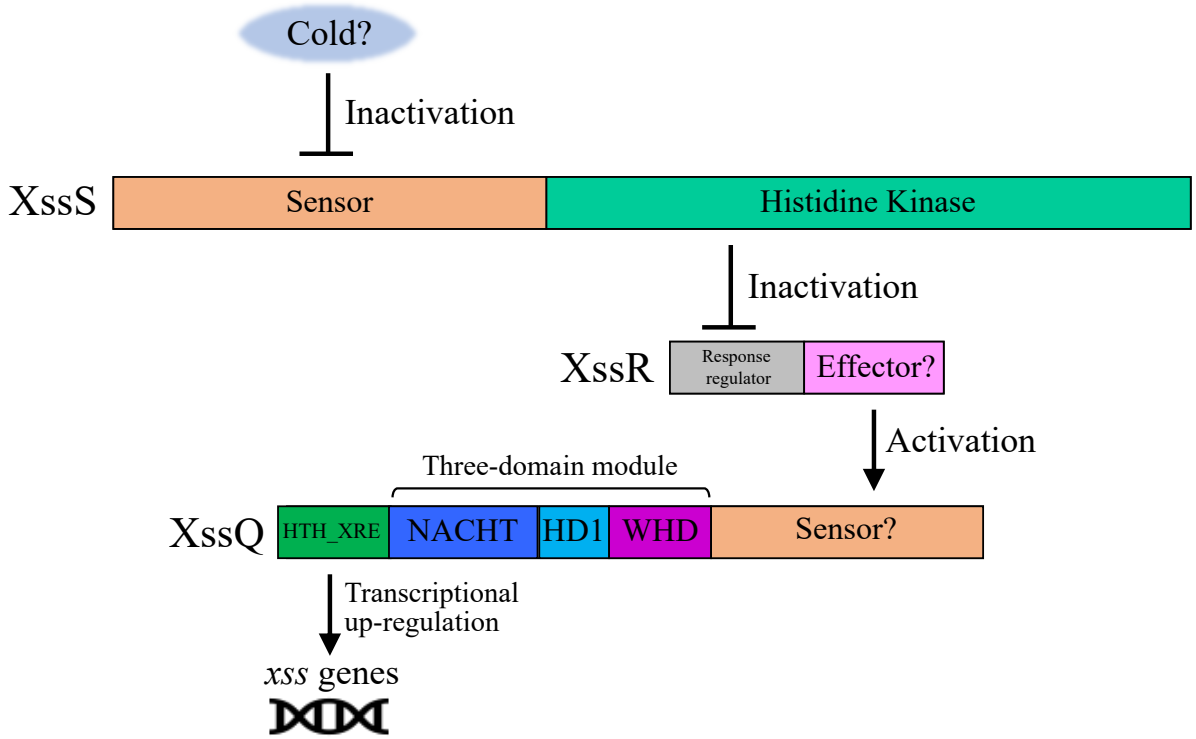

Figure S5. Domain architecture and proposed signal transduction pathway for XssS/XssR/XssQ. Hybrid-type histidine kinase XssS presumably senses a cold signal and transduces it to the response regulator XssR, which in turn activates the transcription of *xss* genes via the STAND protein XssQ. Generally, STAND proteins consist of the three-domain module, sensor region, and effector region[13]. In XssQ, the three-domain module consisting of the NACHT (NAIP [neuronal apoptosis inhibitor protein], CIIA [MHC class II transcription activator], HET-E, and TP1 [mammalian telomerase-associated proteins]) domain (PF05729), HD1 (helical domain 1), and WHD (winged helix domain) responds to a signal from XssR and oligomerizes, leading to the activation of the N-terminal effector domain (helix-turn-helix XRE family domain [SM00530]).

231 analysis of gene expression in Δ*xssS* revealed a tendency for slight upregulation of *xssB*, *xssE*, *xssN*, and

232 *xssP*. We performed RNA-seq analysis of WT, Δ*xssS*, and Δ*xssQ* to see the transcriptome (Fig. S6). The

233 genes down-regulated in Δ*xssQ* and up-regulated in Δ*xssS* were mostly *xss* genes. In detail, the regulated

234 genes were *xssA-E* and *xssL-P*, which were roughly consistent with the qPCR analysis. We conclude

235 that *xssA-E* and *xssL-P* were specifically regulated by XssS/XssR/XssQ. In a previous report, *xssA–xssE*

236 and *xssL–xssP* were up-regulated at low temperature in another substrain of *Synechocystis* 6803 (*Kopf*

237 *et al., 2014b*). To test this in our substrain, we measured the sulfated EPS accumulation of WT culture

238 at 20°C, and it was 3.1-fold greater than that at normal growth temperature (31°C; Fig. 2D, E and Table

239 S2). This result suggests that XssS/XssR/XssQ is a unique temperature sensor for *xss* gene expression.

240 We aligned nucleotide sequences near the transcription start sites of the regulated genes (*xssA,*

241 *xssE, xssL, xssN,* and *xssP*) to find the consensus sequences for XssQ binding (Fig. 3B), according to

242 the differential RNA-seq-type transcriptomic analysis of *Synechocystis* 6803 (*Kopf et al., 2014b*). There

243 are single or tandem consensus sequence, AAGTTXXAC. To confirm the binding of XssQ to this region,

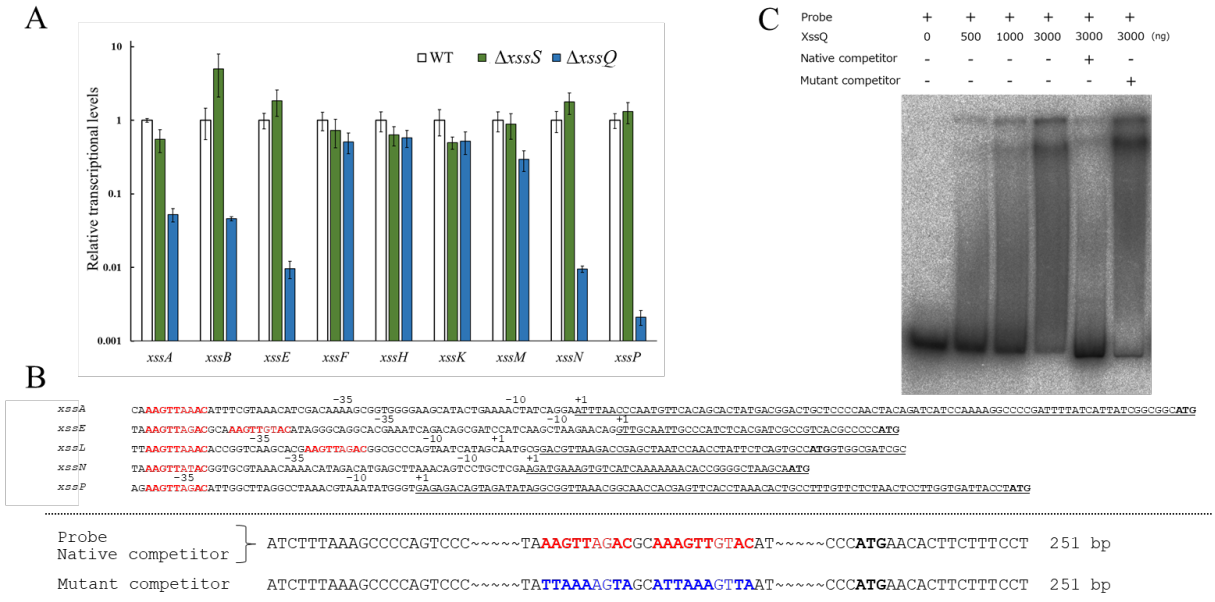

Figure 3 Transcriptional regulation of *xss* genes.

A, Transcript levels for *xss* genes in WT, Δ*xssS*, and Δ*xssQ* measured by qPCR. The internal standard was *rnpB*. Relative expression levels were obtained by normalization to the transcript levels of each gene in WT. Error bars represent SD (n = 3, biological triplicates). **B**, upper; Sequence comparison of upstream regions of the five regulated genes. Putative consensus regions are shown in red and fully conserved nucleotides are shown in bold letter. Underlines represent transcribed regions based on the report(*Kopf et al., 2014b*) and initiation codons of regulated genes are shown in black/bold letters. **B**, lower: Sequences of DNA probe and competitors for *xssE* (native and mutant) used for EMSA of C. Consensus regions are shown in red, and mutated region are shown in blue. Total DNA size is 251 bp, where identical sequences are mostly not shown except 20 bp at both ends. **C,** The autoradiogram image of EMSA of XssQ protein and the DNA probe of *xssE* with some competitors.

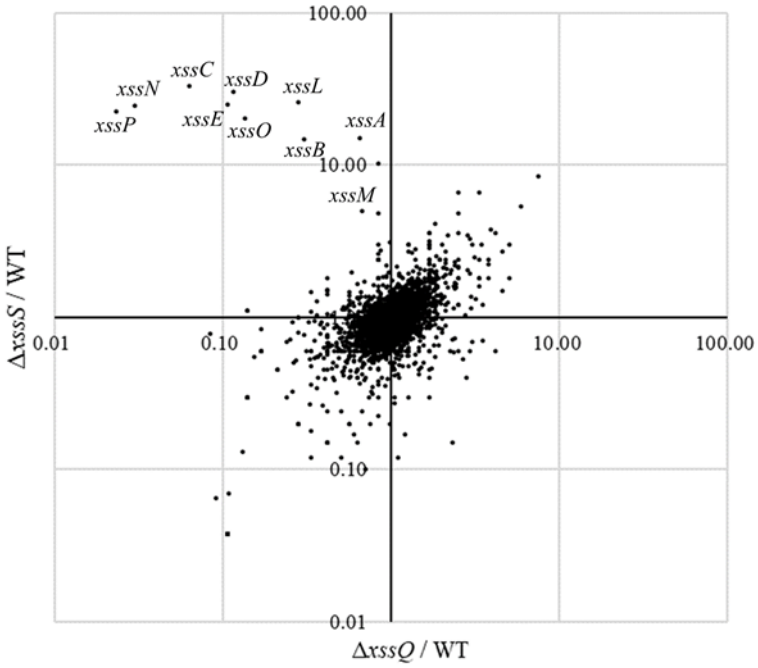

Figure S6. Scatter plot of transcriptome comparison among WT, Δ*xssS*, and Δ*xssQ*. Transcriptional levels were based on RPKM (Reads Per Kilobase of exon per Million mapped reads) value shown in supplementally data 1.

we performed electrophoretic mobility shift assay (EMSA) using purified recombinant XssQ protein and a PCR-amplified DNA fragment of *xssE* upstream (Fig. 3C). The band position of the radiolabeled probe DNA shifted reflecting the concentration of XssQ. This shift was largely eliminated by excess addition of the unlabeled native competitor, but not by addition of the mutant competitor with mutations in the consensus region. These results suggest that XssQ recognizes the consensus sequence of *xssE* and other target genes for their transcriptional activation.

The chemical composition of the sulfated EPS

EPS of WT and the 19-fold overproduction mutant (Δ*xssS*) were subjected to chemical composition analysis (Table 1, Fig. S7). EPS from WT included various sugars and some sulfate groups, whereas EPS from Δ*xssS* consisted of only four types of sugars and sulfate groups with the near stoichiometric molar ratio of rhamnose:mannose:galactose:glucose:sulfate of 1:1:1:5:2. This finding roughly fits with the gene number, i.e., eight glycosyltransferase genes and two sulfotransferase genes.

We speculated that the overaccumulation of EPS in Δ*xssS* reflects the true product of the *xss* cluster. The EPS from WT may contain a considerable amount of unrelated polysaccharides, which were erroneously recovered together with the *xss* product. Here, the sulfated EPS produced by the *xss* cluster in *Synechocystis* 6803 was designated "Synechan".

The OPX protein for synechan biosynthesis

There is no candidate gene in the *xss*-carrying plasmid for the OPX protein of the Wzx/Wzy system, whereas *sll1581*, an OPX homolog, was found on the main chromosome. Disruption of *sll1581* (Δ*sll1581*) abolished bloom formation and EPS accumulation (Fig. 2D, E). Thus, the chromosomal OPX protein Sll1581 (XssT) appears to serve as the outer-membrane exporter for synechan. Interestingly, *Synechocystis* 6803 possesses *xssT* (OPX gene) and *sll0923* (a second PCP-2a gene) on the main chromosome and *xssK* (PCP-2a gene) on the plasmid pSYSM, whereas its close relative *Synechocystis* 6714 harbors only homologs of *sll0923* and *xssT* but lacks the entire plasmid carrying the *xss* cluster.

288 **Table 1.** Chemical composition of the EPS from WT *Synechocystis* 6803 and Δ*xssS* mutant.

	Sugars											*Sulfate residues*
	Neutral sugars (mol/mol %)								Uronic acids (mol/mol %)			Substitution degree
	Rhamnose	Ribose	Mannose	Fucose	Galactose	Xylose	Glucose	Total	Galacturonic acid	Glucuronic acid	Total	(mol/mol %)
WT	16.6	N.D.	25.7	16.2	4.7	10.6	23.1	96.9	N.D.	3.1	3.1	10.4
Δ*xssS*	13.1	N.D.	14.2	1.2	12.5	1.0	57.9	99.9	N.D.	0.1	0.1	26.6

289

290

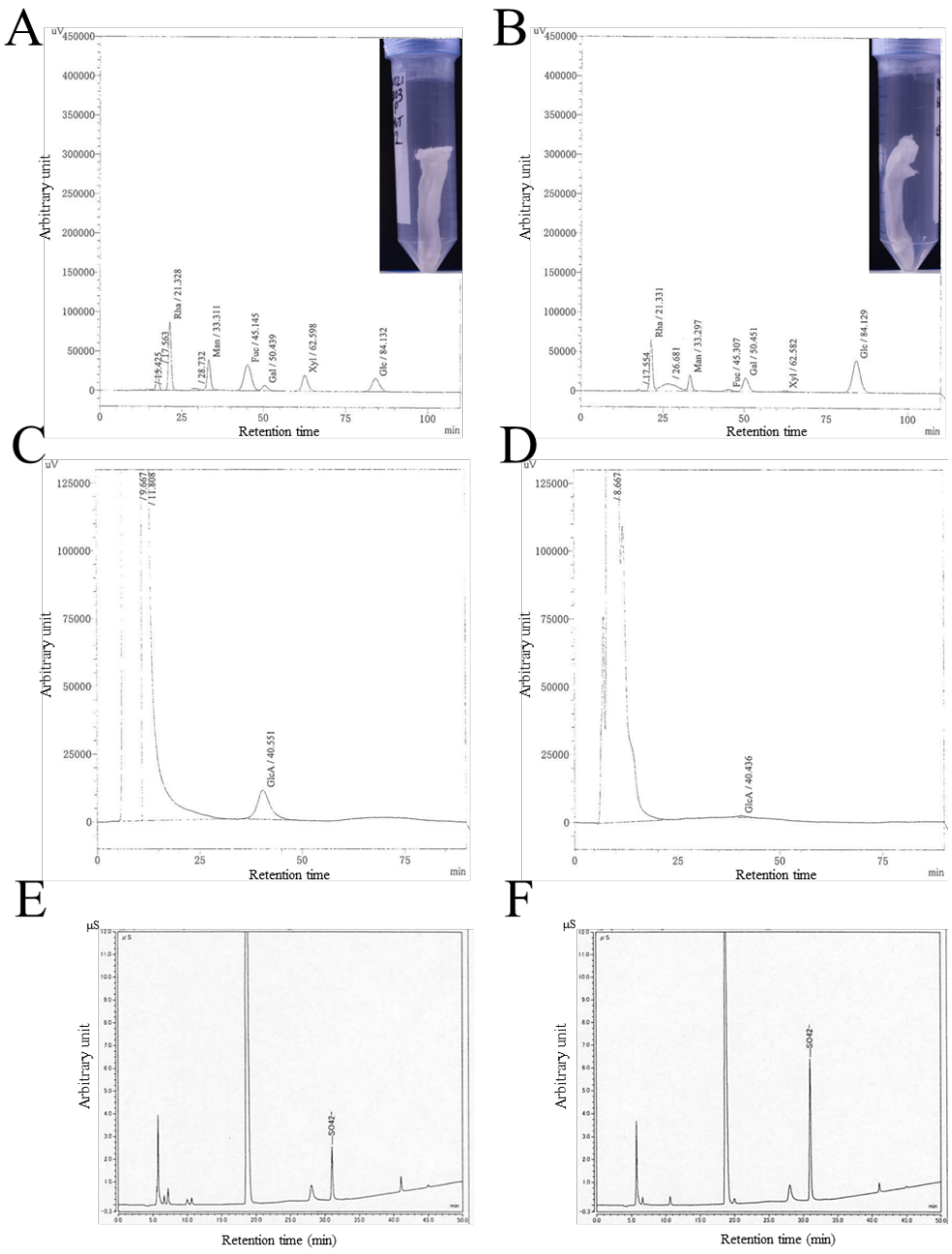

Figure S7. Chromatograms of HPLC and anion exchange column chromatography of EPS. **A** and **B**, HPLC profiles for neutral sugars in wild-type EPS (A) and Δ*xssS* EPS (B). **c** and **d**, HPLC profiles for uronic acids in wild-type EPS (C) and Δ*xssS* EPS (D). The corresponding monosaccharide and retention time are noted at each peak. **E** and **F**, HPLC profiles for SO_4^{2-} after hydrolysis of EPS samples of wild-type (E) and Δ*xssS* (F).

297 This suggested that XssT serves as an OPX for dual function for both XssK and Sll0923. It is likely that

298 *Synechocystis* 6803 acquired pSYSM and borrowed the chromosomal OPX gene *xssT* to produce

299 synechan or, alternatively, *Synechocystis* 6714 may have lost the plasmid.

300

301 **Discussion**

302 Summarizing these data, we propose models for synechan biosynthesis apparatus including

303 OPX and temperature-responsive regulation (Fig. 4A, B and Fig. S5). The model of the Xss apparatus

304 fits well with the known Wzx/Wzy-dependent apparatus represented by xanthan biosynthesis in

305 *Xanthomonas campestris* (*Katzen et al., 1998*). The eight glycosyltransferases including XssP (the

306 priming glycosyltransferase) produce oligosaccharide repeat unit of eight sugars, which is consistent

307 with the sugar composition of synechan. These findings suggest that the *xss* cluster on the pSYSM

308 plasmid harbors a whole set of genes for synechan biosynthesis except the OPX gene (*xssT* on the main

309 chromosome). Notably, the cluster harbors two sulfotransferase genes, which have not been found to

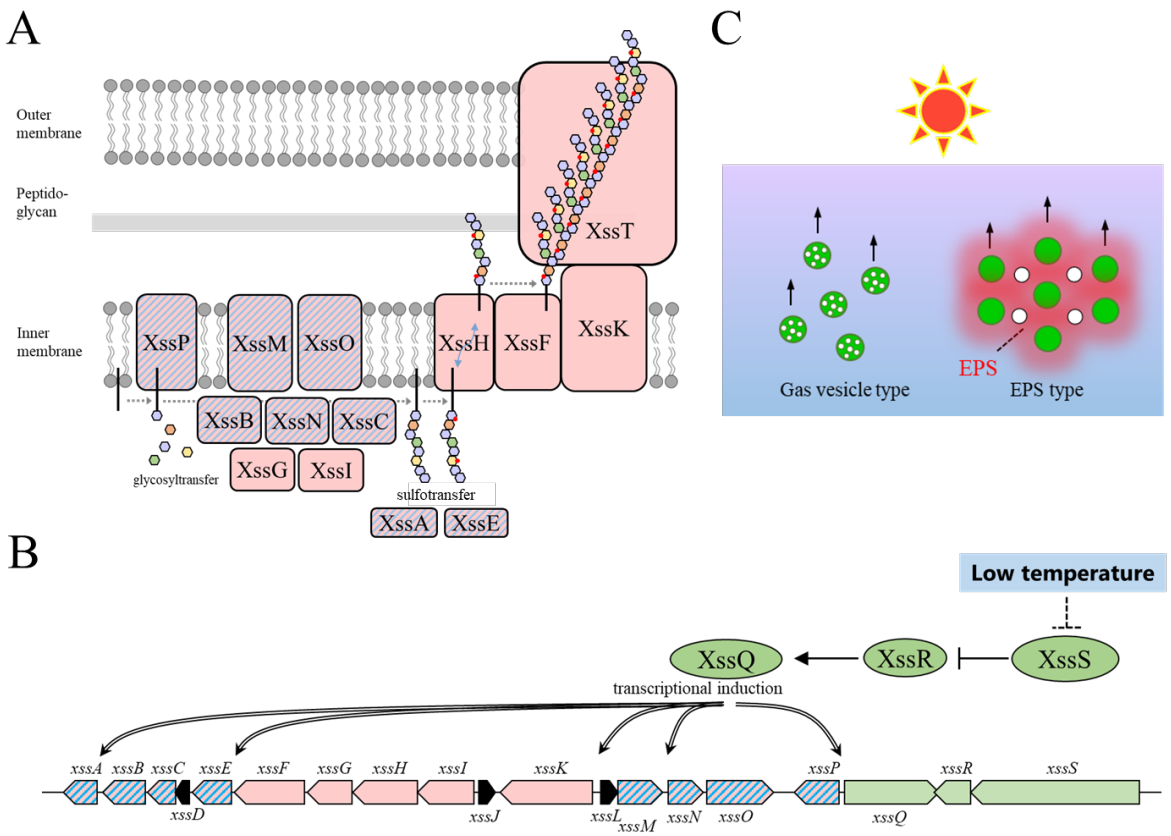

Figure 4 Proposed models for the synechan biosynthesis apparatus, transcriptional regulation, and bloom formation.

A, Model for the synechan biosynthesis apparatus with sugar polymerization and modification. Red boxes represent biosynthesis components, and red boxes with blue stripes represent transcriptionally regulated components. A putative lipid linker is shown as a black rod. Each monosaccharide is shown as a small hexagon, and each sulfate group is shown as a red spot. **B,** Signaling and transcriptional regulation model. Green arrows and ellipses represent regulatory genes and proteins, respectively. Genes for synechan biosynthesis are shown in red, and transcriptionally regulated genes are depicted with blue stripes. Arrows with double lines represent transcriptional activation. **C,** Two flotation models for bloom formation in cyanobacteria. Left, flotation of cells (green circles) with intracellular gas-filled vesicles (white circles). Right, flotation of EPS (red shading)-entrapped cells (green circles) and extracellular gas bubbles (white circles), which are generated by photosynthesis.

our knowledge in other bacterial gene clusters for extracellular polysaccharide biosynthesis. Sulfotransferases, XssA and XssE, belong to distinct subfamilies of bacterial sulfotransferases. We found many sulfotransferase genes in various cyanobacterial genomes by Pfam search (PF00685, PF03567, PF13469). They are mostly found in gene clusters for putative extracellular polysaccharide biosynthesis (Wzx/Wzy-type and ABC-type) (Fig. S8). It should be noted that they are more or less partial as a cluster for extracellular polysaccharide biosynthesis system, whereas the *xss* cluster appears to be complete except the OPX gene in *Synechocystis* 6803. It is well established that the polysaccharide moiety of membrane-anchored lipopolysaccharides and CPS of bacteria are produced and exported by the Wzx/Wzy-dependent or ABC transporter–dependent pathways, whereas free EPS, i.e., xanthan and cellulose, are produced by the Wzx/Wzy-dependent and synthase-dependent pathways but not by the ABC transporter–dependent pathway (*Schmid et al., 2015, Willis and Whitfield, 2013*). In the literature, a sulfated CPS was reported in *Arthrospira platensis* (formerly *Spirulina platensis*) (*Mouhim et al., 1993*). This sulfated CPS may be produced by an ABC transporter-type gene cluster in Fig. S8. Gene

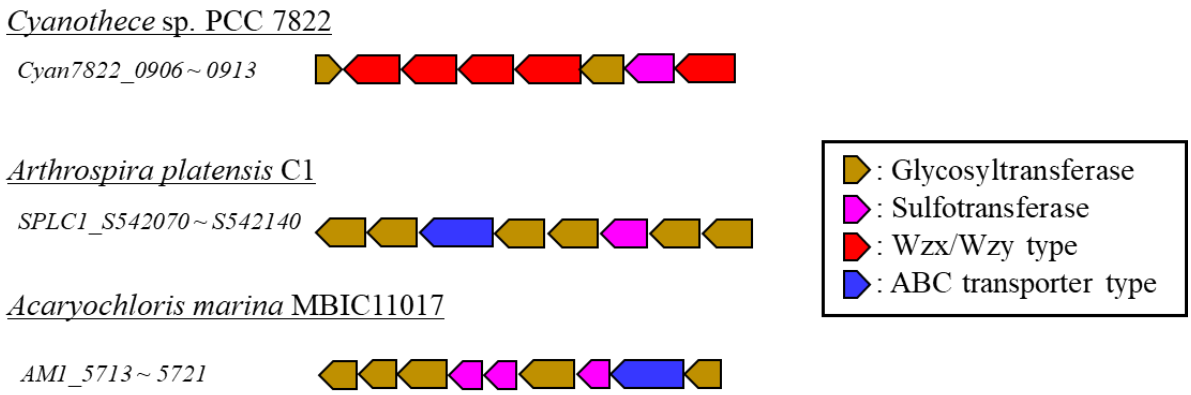

337

338 **Figure S8.** Typical examples of putative gene clusters for biosynthesis of sulfated polysaccharides in

339 cyanobacteria.

340 A part of each cluster harboring genes for sulfotransferases, glycosyltransferases, and polysaccharide

341 biosynthesis/export systems (Wzx/Wzy type and ABC transporter type) in cyanobacterial genomes.

342

disruption will confirm such predictions deduced from the gene cluster analyses, although targeted disruption is not so easy in many cyanobacteria due to poor transformation efficiency except *Synechocystis* 6803. In contrast, no sulfated polysaccharide has been reported in the other bacteria, though many sulfotransferases are also registered in Pfam database. Some of them are known to transfer a sulfuryl group to lipo-oligosaccharides in rhizobia (Nod factor) and mycobacteria (*Mougous et al., 2002*).

XssQ, a STAND protein with a DNA binding domain is indeed the transcriptional activator for *xssE* and other induced genes. XssQ homologs are found widely throughout the cyanobacteria but the set of XssS/XssR/XssQ is found near the gene cluster for sulfated EPS biosynthesis with sulfotransferases in many cyanobacteria (Fig. S9, Table S3). Consensus sequences are also found in upstream of some genes in the cluster, suggesting that the XssS/XssR/XssQ system may operate universally for induction of sulfated EPS production under certain environmental conditions such as cold temperature.

355 Acidic polysaccharides containing uronic acids and other carboxylic groups are common in
356 bacteria, but sulfated polysaccharides are produced exclusively by cyanobacteria (*Pereira et al., 2009*).
357 To speculate on the physiological significance of sulfated polysaccharides, we summarized the
358 distribution of sulfotransferase genes in cyanobacteria of various habitats (Table S3). Species living in
359 high salinity environments such as a salt lake or seawater mostly produce sulfated polysaccharides. The
360 freshwater species *Synechocystis* sp. PCC 6714 lacks the *xss* genes including sulfotransferases and salt-
361 resistance genes that are present in the more salt-resistant *Synechocystis* 6803 (*Kopf et al., 2014a*). A
362 cyanobacterial sulfated polysaccharide, sacran, shows much higher capacity for saline absorption than
363 does hyaluronic acid, a uronic acid–containing polysaccharide, whereas both absorb pure water
364 efficiently (*Okajima et al., 2008*). The wide distribution of sulfated polysaccharides among many
365 cyanobacteria may reflect their inherent compatibility with survival in some saline environments.
366 There are many putative genes that may be involved in biosynthesis and export of
367 extracellular polysaccharides and lipopolysaccharides in the genome of *Synechocystis* 6803

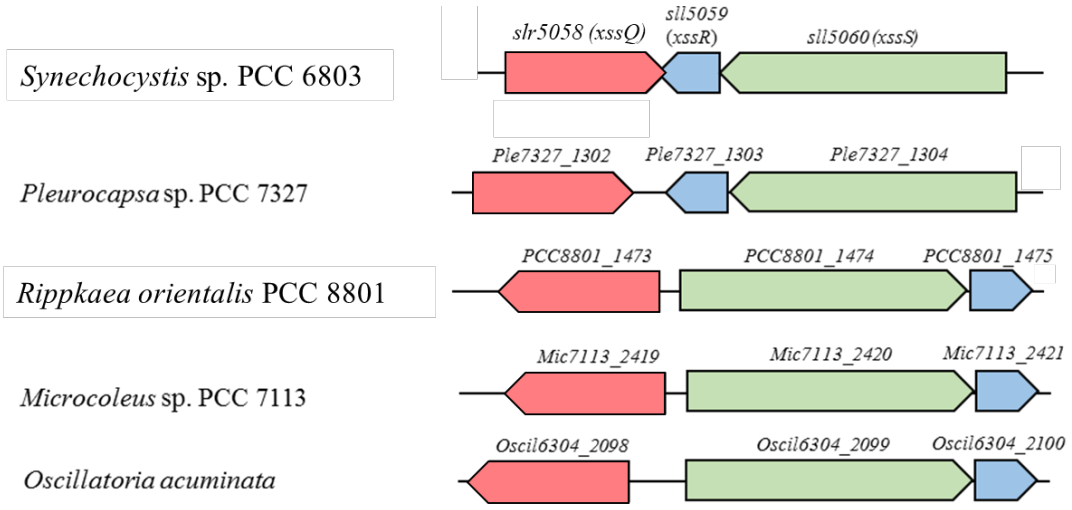

Figure S9. Homologous gene clusters of *xssS*/*xssR*/*xssQ* in some cyanobacteria. The colored blocks indicate genes with direction. The homologs of each gene are represented by their corresponding colors (red, *xssQ*; blue, *xssR*; green, *xssS*).

373 **Table S3.** Number of sulfotransferase genes (STs) in the genome of cyanobacteria collected from various

374 habitats.

Habitat	Species	STs	Comment
Marine	*Trichodesmium erythraeum* IMS101	30	
Marine	*Crocosphaera subtropica* ATCC 51142	14	Formerly *Cyanothece* sp. ATCC 51142
Marine	*Acaryochloris marina* MBIC 11017	13	
Marine	*Synechococcus* sp. WH8102	12	
Marine	*Pseudanabaena* sp. PCC 7367	8	
Marine	*Rivularia* sp. PCC 7116	5	
Marine	*Synechococcus* sp. PCC 7002	4	
Marine	*Prochlorococcus marinus* MIT 9313	2	
Marine	*Nodularia spumigena* UHCC 0039	0	
Salt lake	*Arthrospira platensis* NIES-39	16	
Salt lake	*Acaryochloris* sp. CCMEE 5410	6	
Terrestrial (rice field)	*Gloeothece verrucosa* PCC 7822	17	Formerly *Cyanothece* sp. PCC 7822
Terrestrial (rice field)	*Rippkaea orientalis* PCC 8801	8	Formerly *Cyanothece* sp. PCC 8801
Terrestrial (rice field)	*Cyanothece* sp. PCC 7425	6	
Terrestrial	*Gloeobacter violaceus* PCC 7421	10	
Terrestrial	*Oscillatoria nigro-viridis* PCC 7112	10	
Terrestrial	*Leptolyngbya* sp. PCC 7376	8	
Terrestrial	*Oscillatoria acuminata* PCC 6304	6	
Terrestrial	*Cylindrospermum stagnale* PCC 7417	3	
Terrestrial	*Microcoleus* sp. PCC 7113	2	
Terrestrial	*Crinalium epipsammum* PCC 9333	2	
Terrestrial	*Nostoc punctiforme* NIES-2108	1	
Terrestrial	*Nostoc* sp. HK-01	1	
Terrestrial	*Nostoc punctiforme* PCC 73102	0	
Terrestrial	*Chroococcidiopsis thermalis* PCC 7203	0	
Hot spring	*Pleurocapsa* sp. PCC 7327	10	
Hot spring	*Thermoleptolyngbya* sp. O-77	7	
Hot spring	*Thermosynechococcus elongatus* BP-1	0	
Hot spring	*Thermosynechococcus vulcanus* NIES-2134	0	
Hot spring	*Synechococcus* sp. JA-3-3Ab	0	
Fresh water	*Aphanothece sacrum*	11	Sacran *(Okajima et al. , 2008)*
Fresh water	*Microcystis aeruginosa* NIES-843	9	
Fresh water	*Synechocystis* sp. PCC 6803	2	Salt tolerant *(Kopf et al. , 2014a)*
Fresh water	*Synechocystis* sp. PCC 6714	0	Salt sensitive *(Kopf et al. , 2014a)*
Fresh water	*Anabaena cylindrica* PCC 7122	4	
Fresh water	*Calothrix* sp. PCC 7507	3	
Fresh water	*Synechococcus elongatus* PCC 7942	0	Salt sensitive
Fresh water	*Nostoc (Anabaena)* sp. PCC 7120	0	
Fresh water	*Leptolyngbya boryana* IAM M-101	0	
Fresh water	*Anabaena variabilis* ATCC 29413	0	
Fresh water	*Calothrix* sp. PCC 6303	0	
Fresh water	*Calothrix* sp. 336/3	0	

375

376

377 (*Fisher et al., 2013, Pereira et al., 2015*). Many of them have been disrupted for characterization. With

378 regard to the Wzx/Wzy-dependent system, *sll5052* (*xssK*) disruption mutant showed no clear phenotypes

379 for bloom formation or EPS production (*Jittawuttipoka et al., 2013*), probably because the parent strain

380 did not produce discernable amount of EPS like our nonmotile strain. Similarly, the deletion mutant of

381 *sll5049* (*xssH*) did not show any defect in EPS or CPS accumulation, though related mutants (Δ*sll0923*

382 for a second PCP-2a) were shown to be depleted slightly of both CPS and EPS (*Pereira et al., 2019*).

383 These results contrast with our null phenotype of Δ*sll5052* (*xssK*) and Δ*sll5049* (*xssH*), probably because

384 of the difference in the parent strains. In addition, we found that our Δ*sll0923* did not show any defect

385 in the bloom formation. On the other hand, disruption of *sigF* (*slr1564*) for a sigma factor of global cell

386 surface regulation increased three to four fold accumulation of sulfated EPS (*Flores et al., 2019a, Flores*

387 *et al., 2019b*). The proteome analysis of Δ*sigF* revealed many (more than 160) proteins except for any

388 Xss proteins were up-regulated, leaving the sulfated EPS biosynthesis pathway elusive. The sugar

389 composition of the sulfated EPS of their WT is similar to our WT, although the composition of EPS of

390 Δ*sigF* was different for WT or synechan from our Δ*xssS*.

391 To get insights into the difference in bloom formation between the motile and nonmotile
392 substrains, we compared transcription data (Table S4). It is evident that many *xss* genes on the plasmid
393 are expressed several times higher in the motile substrain than the nonmotile one except for *xssT* on the
394 main chromosome, despite that the nucleotide sequence of the *xss* gene cluster was completely
395 conserved between them. This fact suggests a possibility that another mechanism besides the
396 XssS/XssR/XssQ contributes to the difference between the substrains. For example, the plasmid copy
397 number of pSYSM may be higher in the motile substrain than the nonmotile substrain. The plasmid
398 function is often affected depending on variations in the main chromosome (*Vial and Hommais, 2020*).
399 Anyway, it is very important to select the parent strain depending on the research purpose.

400 The cyanobacterial bloom rapidly accumulates in populations of cyanobacterial cells floating
401 on the water surface, which often produce potent cyanotoxins (hepatotoxins, neurotoxins, etc.) (*Merel*
402 *et al., 2013*). Blooms are thought to be supported mainly by cellular buoyancy due to intracellular

403 **Table S4.** Transcriptional levels of *xss* genes in the motile (WT) and nonmotile (NM) substrains.

locas tag	gene name	WT (RPKM)	NM (RPKM)	WT / NM
sll5042	*xssA*	46.7	28.5	1.6
sll5043	*xssB*	43.2	9.8	4.4
sll5044	*xssC*	53.3	4.5	12.0
ssl5045	*xssD*	77.6	6.2	12.4
sll5046	*xssE*	291.8	24.0	12.1
sll5047	*xssF*	17.9	8.7	2.1
sll5048	*xssG*	71.7	28.9	2.5
sll5049	*xssH*	41.8	21.3	2.0
sll5050	*xssI*	26.8	33.6	0.8
slr5051	*xssJ*	231.6	112.0	2.1
sll5052	*xssK*	29.0	23.7	1.2
slr5053	*xssL*	43.9	6.5	6.8
slr5054	*xssM*	33.2	22.5	1.5
slr5055	*xssN*	455.5	14.4	31.6
slr5056	*xssO*	120.5	23.3	5.2
sll5057	*xssP*	514.1	12.6	40.9
slr5058	*xssQ*	54.3	27.5	2.0
sll5059	*xssR*	40.5	45.9	0.9
sll5060	*xssS*	12.8	11.7	1.1
sll1581	*xssT*	133.3	181.8	0.7

404

405 Transcriptional level is given as RPKM (Reads Per Kilobase of exon per Million mapped reads).

406

407 proteinaceous gas vesicles constructed by gas vesicle proteins (*Beard et al., 2002, Walsby, 1994*).

408 Moreover, recent studies suggested that extracellular polysaccharides are also important for the bloom

409 formation (*Chen et al., 2019*). Some papers reported that the cells without gas vesicle can form blooms

410 by EPS-dependent manner after artificial addition of divalent cations (Ca^{2+} or Mg^{2+}) (*Dervaux et al.,*

411 *2015, Wei et al., 2019*). On the other hand, our study demonstrated that the gas-trapped EPS is sufficient

412 for bloom formation of *Synechocystis* 6803, which does not produce gas vesicles, without addition of

413 any divalent cations. This result is consistent with reports that cyanobacteria without gas vesicles form

414 booms in natural environments, including freshwater lakes (*Casero et al., 2019, du Plooy et al., 2015,*

415 *Steffen et al., 2012*).

416 Finally, sulfated polysaccharides are expected to be healthy foods, industrial materials and

417 medicines (*Jiao et al., 2011, Wardrop and Keeling, 2008*). Some sulfated EPS from *Synechocystis* 6803

418 showed antitumor activity (*Flores et al., 2019a*), though this EPS may not be identical to synechan. The

419 Xss-dependent biosynthesis of synechan in *Synechocystis* 6803 should be a good model for studies of

other cyanobacterial sulfated polysaccharides. Combinatorial expression of sulfotransferases and glycosyltransferases from other cyanobacteria in *Synechocystis* cells will provide clues to their functions. Heterologous expression of *Synechocystis xss* genes in other organisms will also open a possibility of large scale production of modified synechan species. Further molecular studies of *xss* genes and related genes from the database should accelerate screening and potential applications of cyanobacterial sulfated polysaccharides.

426 **Materials and Methods**

427 ***Cyanobacterial strains and cultures***

428 The motile substrain PCC-P of the unicellular cyanobacterium *Synechocystis* sp. PCC 6803,

429 which exhibits phototaxis (*Yoshihara et al., 2000*) and forms bloom-like aggregates, was used as the

430 WT in this work. A non-motile glucose-tolerant substrain, which has been widely used for studies of

431 photosynthesis, was used for comparison (*Chin et al., 2018*). Cells were maintained in BG11 liquid

432 medium (*Stanier et al., 1971*) under continuous illumination with bubbling of 1% CO_2 in air at 31°C, or

433 on 1.5% agar plates. White light of 30 μmol photons $m^{-2}s^{-1}$ was generated by fluorescent lamps. Cell

434 density was monitored at 730 nm.

435

436 ***Construction of plasmids and mutants***

437 Primers used are listed in Table S5. Plasmids and mutants were constructed as described

438 (*Chin et al., 2018*). In brief, the DNA fragments, antibiotic-resistance cassettes, the *trc* promoter, and

439 plasmid vectors were amplified by PCR using PrimeSTAR MAX DNA polymerase (Takara, Shiga,
440 Japan) and combined using the In-Fusion System (Takara). The resulting plasmid constructs were
441 confirmed by DNA sequencing.

442 Gene disruption was performed in two different ways. One method was replacement of a
443 large portion of a targeted gene(s) with an antibiotic resistance cassette. The other method was
444 replacement of the translation initiation codon with a stop codon. In both cases, the screening cassette
445 without the terminator was inserted in the direction of the targeted gene(s) to allow transcriptional
446 readthrough of the downstream gene(s). For overexpression, gene expression was constitutively driven
447 by the strong *trc* promoter in two ways: integration of a target gene with the strong *trc* promoter into a
448 neutral site near *slr0846* or IS203c, or replacement of the target-gene promoter with the *trc* promoter.
449 Natural transformation and subsequent homologous recombination were performed as described(*Chin*
450 *et al., 2018*). The antibiotic concentration for the selection of transformants was 20 $\mu g \cdot mL^{-1}$
451 chloramphenicol, 20 $\mu g \cdot mL^{-1}$ kanamycin, and/or 20 $\mu g \cdot mL^{-1}$ spectinomycin. Complete segregation of

452 **Table S5.** Primer sequences.

Product (purpose)	Primer name	Sequence (5' => 3')
Antibiotic resistance cassette	Sp-1F	ATGCGCGAAGCCGTGATTGCC
	Sp-2R	TAGTAAAGCCCTCGCTAG
	Km-1Fup	AATTCCCCTGCTCGCGCTGCCGCAAGCACTCAGGG
	Km-2Rcom	AATATTGCGAAGCGGCCAACCTTTCATAGAAGGCG
	Cm-1Fup	AATTCCCCTGCTCGCGCAGCGCTGATGTCCGGCGGTGCT
	Cm-2Rcom	AATATTGCGAAGCGGCTAACCGTTTTTATCAGGC
Glycosyltransferase disruption	slr1943-1FpS	AACGACGGCCAGTGAAGACCGCATGTGTGGCAGT
	slr1943-2Rup	GCGAGCAGGGGAATTGGCTTGGTGAATTTGTAACC
	slr1943-3Fcom	CCGCTTCGCAATATTGGCTGGCTTTGAACAACTTC
	slr1943-4RpS	AAACAGCTATGACCAATCGGCAATGTAGGTGAAGG
	slr1943-5F	AAGCCCGTCTGGAGTTTG
	slr1943-6R	AATCCGGGTCGATGGTAC
	slr1063-1FpS	AACGACGGCCAGTGAATGTCCAAAAATGACAAGC
	slr1063-2Rup	GCGAGCAGGGGAATTACACGATTGGCGGAAATTTC
	slr1063-3Fcom	CCGCTTCGCAATATTCTGGTATATCAGATTACTCG
	slr1063-4RpS	AAACAGCTATGACCAGCTTGGAGTAAGCTGCATAA
	slr1063-5F	ATGCGTCGTTTCGGTCAC
	slr1063-6R	TGCAAGACATTCCCGGAC
	sll0501-1FpS	AACGACGGCCAGTGAGGGATTAGGCAGGGGTAATA
	sll0501-2Rup	GCGAGCAGGGGAATTCCTGTCAATTTAGTCAGTGC
	sll0501-3Fcom	CCGCTTCGCAATATTGACCATTGAACTGTCTATTGTG
	sll0501-4RpS	AAACAGCTATGACCAGGTCAGAATCGATACCATGG
	sll0501-5F	TCAAAGGGAACGTGCTGG
	sll0501-6R	GTTGCCTTGGGCGTAATC
	slr1118-1FpS	AACGACGGCCAGTGATCCTGCCGCTCAAAGTATTC
	slr1118-2Rup	GCGAGCAGGGGAATTCGATCGCCGCTTTAGCTAAA
	slr1118-3Fcom	CCGCTTCGCAATATTTCAAGCTCCCCGTTGGTTAA
	slr1118-4RpS	AAACAGCTATGACCAGCAGGGGAAATCGTTTGCAT
	slr1118-5F	CGCACCATTATCAGCACG
	slr1118-6R	ATCGCTTCGGTTCCATGC
	sll5052_54-1FpS	AACGACGGCCAGTGATCGCTGTTTGTTTGGTGAGG
	sll5052_54-2Rup	GCGAGCAGGGGAATTCAATGCTGGCTTGGCCAAATTA
	sll5052_54-3Fcom	CCGCTTCGCAATATTGCTGCTGGATTCAGGAATTG
	sll5052_54-4RpS	AAACAGCTATGACCACAGGCGGGAGATTGCTAAAA
	sll5052_54-5F	GGTACTTCGCTGTAGTTC
	sll5052_54-6R	GGGCAAAACTTCGTCTTC
xss gene disruption and overexpression	xssA-1FpS	AACGACGGCCAGTGACCCCAGCTTGTAGTGGATTG
	xssA-2Rup	GCGAGCAGGGGAATTTTCATGCCGCCGATAATGAT
	xssA-3Fcom	CCGCTTCGCAATATTAGAAATGTGCCACCAGTACCC
	xssA-4RpS	AAACAGCTATGACCAATCTAGGTTCGACCCCTACC
	xssA-5Ftrc	GAGGAATAAACCATGAAATGTGCCACCAGTACC
	xssA-6F	GATCGCCAATGGCAAGAT
	xssA-7R	ATTGGGTTCCTTCAGCGA
	xssB-1FpS	AACGACGGCCAGTGAGAGCGTGTTTGAAAAGCCCC
	xssB-2Rup	GCGAGCAGGGGAATTGGCCATAATCTTGCAAATACTC
	xssB-3Fcom	CCGCTTCGCAATATTAGGCCATAATTGCTTCAAACAATAG
	xssB-4RpS	AAACAGCTATGACCAGAAATTCTACTCCGGACGGT
	xssB-5Ftrc	GAGGAATAAACCATGGCCATAATTGCTTCAAACAA
	xssB-6F	GCCAACAAAATCCCCAGA
	xssB-7R	AATCCACTACAAGCTGGG
	xssC-1FpS	AACGACGGCCAGTGAAGGCTACTGGGTTTGAGGTT
	xssC-2Rup	GCGAGCAGGGGAATTATCATTTCCCGACGGCGATC
	xssC-3Fcom	CCGCTTCGCAATATTAGATCCAAGAGTTTCAGCGGTT
	xssC-4RpS	AAACAGCTATGACCACCGCACAATGGTATCGCTAT
	xssC-5F	CATTACTTTTTCCCCGCC
	xssC-6R	CCGCTGTAAAAAATGCAGC

453

454

455 **Table S5.** Continuing.

Product (purpose)	Primer name	Sequence (5' => 3')
xss gene disruption and overexpression	xssE-1FpS	AACGACGGCCAGTGACCGTCGAGCGAGTTAAGG
	xssE-2Rup	GCGAGCAGGGGAATTAAGTGTTCATGGGGGCGTGA
	xssE-3Fcom	CCGCTTCGCAATATTTAGAACACTTCTTTCCTCGAAT
	xssE-4RpS	AAACAGCTATGACCAGCTCTTAGGGCGGGGAAAA
	xssE-5Ftrc	AAGGAGGAATAAACCATGAACACTTCTTTCCTCGAAT
	xssE-6F	TAGTGAGCAGGGGAAACT
	xssE-7R	CACTTACCTGATCGATGAC
	xssF-1FpS	AACGACGGCCAGTGACTGCAAAAACGAGGCCATGA
	xssF-2Rup	GCGAGCAGGGGAATTGTCATGGATCGTTTGCTGTTG
	xssF-3Fcom	CCGCTTCGCAATATTAGACCCCCCAAGCCCAACTG
	xssF-4RpS	AAACAGCTATGACCAATAGACCCGATTGCGTTTCC
	xssF-5F	CCCATGATGTTGTGGTGT
	xssF-6R	TTGCCTGACCCTGACTTT
	xssG-1FpS	AACGACGGCCAGTGACTCCACGGCATTATTTACCC
	xssG-2Rup	GCGAGCAGGGGAATTCATACTCCTAACTCCATAACGC
	xssG-3Fcom	CCGCTTCGCAATATTAGAAAATCACCTTTGTTTTACCCTA
	xssG-4RpS	AAACAGCTATGACCATCATGGATCGTTTGCTGTTGC
	xssG-5F	ATCTAGCAGTGGCTTACG
	xssG-6R	CCGAAGCCATTGGCTAAT
	xssH-1FpS	AACGACGGCCAGTGAGCTGAAAACCCTCGGCTTAA
	xssH-2Rup	GCGAGCAGGGGAATTCATAGTTACGGCGCCGATG
	xssH-3Fcom	CCGCTTCGCAATATTAGGCTTCCCTCAATAAACTGG
	xssH-4RpS	AAACAGCTATGACCATTGGCAAAGTTACCGATCGC
	xssH-5F	GTAGAAGCAATGCAGTCTG
	xssH-6R	GGTATTTACCAACGCCATC
	xssI-1FpS	AACGACGGCCAGTGACCAATTTGCAACATCCCGAC
	xssI-2Rup	GCGAGCAGGGGAATTTAGCCCCGAATCAATTATCC
	xssI-3Fcom	CCGCTTCGCAATATTAGGTGAGATCGCCCCAATTCC
	xssI-4RpS	AAACAGCTATGACCAAATGTTGCTGCACCATGGC
	xssI-5F	AATTCGGTCTAGCTTGCC
	xssI-6R	GCTCTTCCAAAGCCAGAA
	xssK-1FpS	AACGACGGCCAGTGATCTGCCACTTGGTAAACCTC
	xssK-2Rup	GCGAGCAGGGGAATTGGAATATTCGGGCGCTTTGA
	xssK-3Fcom	CCGCTTCGCAATATTTGGTGCGGGTTTATCTCAAC
	xssK-4RpS	AAACAGCTATGACCAGCAGATTGTTCCGTTTTTGAA
	xssK-5F	CGCTCCCATAAAGATCTC
	xssK-6R	TTCTGGAATCTGGGGGAGAA
	xssM-1FpS	AACGACGGCCAGTGATCGCTGTTTGTTTGGTGAGG
	xssM-2Rup	GCGAGCAGGGGAATTCAATGCTGGCTTGGCCAAAT
	xssM-3Fcom	CCGCTTCGCAATATTCTTCCATGGTGGTTAGTGGA
	xssM-4RpS	AAACAGCTATGACCACAGGCGGGAGATTGCTAAAA
	xssM-5F	CTGATAGGCTGTTGCTAACC
	xssM-6R	GCAGTTGTTTATGGACCCTC
	xssN-1FpS	AACGACGGCCAGTGAGGAATTGTCGTTATTGGGCG
	xssN-2Rup	GCGAGCAGGGGAATTTGGAATTCATTGCTTAGCCC
	xssN-3Fcom	CCGCTTCGCAATATTAGAATTCCATCACGCTTCTCAA
	xssN-4RpS	AAACAGCTATGACCATATAGGACAGGGCGATCTTC
	xssN-5Ftrc	GAGGAATAAACCATGAATTCCATCACGCTTCTCAA
	xssN-6F	TCCGCCTCACCAAACAAA
	xssN-7R	GCCACTTGGTAAACCTCT
	xssO-1FpS	AACGACGGCCAGTGAGTTAGCCTGGCTCTATGCCA
	xssO-2Rup	GCGAGCAGGGGAATTAACACCTAAACGGTCCGAGA
	xssO-3Fcom	CCGCTTCGCAATATTAGTTTCGGGGTTGCCTAGCCAA
	xssO-4RpS	AAACAGCTATGACCAAATAGCGGCTTTCAGCAACC
	xssO-5F	ATGAGCAAAGTCGGGTTG
	xssO-6R	GGAGAATGAAACGAGACC
	xssP-1FpS	AACGACGGCCAGTGACCTCTGCTTCAGATAAAGCTG
	xssP-2Rup	GCGAGCAGGGGAATTGCCATAGGTAATCACCAAGGAG
	xssP-3Fcom	CCGCTTCGCAATATTAGGCTAGCACTATTCAACTGATTG
	xssP-4RpS	AAACAGCTATGACCATTCTCACCCACTCGGGTGTA
	xssP-5Ftrc	GAGGAATAAACCATGGCTAGCACTATTCAACTGA
	xssP-6F	CTGGTGAAGCTTTAAGGG
	xssP-7R	AAAATCGAACACCAGCCG

456

457 **Table S5.** Continuing.

Product (purpose)	Primer name	Sequence (5' => 3')
xss gene disruption and overexpression	xssQ-1Rup	GCGAGCAGGGGAATTGCCATGTTTACAATGATAGAGA
	xssQ-2Fcom	CCGCTTCGCAATATTAGGCAAAACGTTCCCTTAAAGCT
	xssQ-3Ftrc	GAGGAATAAACCATGGCAAAACGTTCCCTTAAAG
	xssQ-4Rrrn	CAGACCGCTTCTGCGTTAGCTAACCTTTTCGCC
	xssR-1FpS	AACGACGGCCAGTGAGGAGGAAGTAGATGGGTTAC
	xssR-2Rup	GCGAGCAGGGGAATTGTCGGAGAAGTCTCAGTCAT
	xssR-3Fcom	CCGCTTCGCAATATTCAGCAATTGCGACAGTTTCC
	xssR-4RpS	AAACAGCTATGACCAACGTTAACAGCGCCGTTGTT
	xssR-5F	CAGACGGAGCAACCTTTT
	xssR-6R	GGAAACTGTCGCAATTGC
	xssR-7Ftrc	GAGGAATAAACCATGACTGAGACTTCTCCG
	xssR-8Rrrn	CAGACCGCTTCTGCGCTACCCCATGACCAGGGC
	xssS-1Rup	GCGAGCAGGGGAATTACCTGCAAAAAGGTTGCTCC
	xssS-2Fcom	CCGCTTCGCAATATTCGGGGGTTGATGGACAATAT
sll1581 disruption	sll1581-1FpS	AACGACGGCCAGTGATGGCTTTTCAGGCAATTCCG
	sll1581-2Rup	GCGAGCAGGGGAATTTTCCAAGTTCAAGGCCACCA
	sll1581-3Fcom	CCGCTTCGCAATATTCAGAGTGAACTCATAACCCA
	sll1581-4RpS	AAACAGCTATGACCATCTGCCTGTAATCTCTGCAC
	sll1581-5F	ATCTGGTGGCCTTGAACT
	sll1581-6R	TTCAGTTGCTTGCAGGCA
RT-qPCR	rnpB-1F	GAGAGTTAGGGAGGGAGTTGC
	rnpB-2R	AAGGGCGGTATTTTTCTGTG
	xssA-8F	TTGCCCACCTACCCTGACAC
	xssA-9R	AGGCGATCGATGGGATGACG
	xssB-8F	CGGCCAGGGGCAATTCAAAC
	xssB-9R	ATTTGGGGAGTGCCATCGGG
	xssE-8F	CAACGCGGCTATGAAGCCAG
	xssE-9R	GCCCCGTAACGCTGTAAACG
	xssF-7F	GCTGGAAACGCAATCGGGTC
	xssF-8R	GTTCAGCAGGCCAAAGGCTC
	xssH-7F	CCGCAATCGCTTTACCTGGG
	xssH-8R	GGCGAGAAAGGTCATGGCTG
	xssK-7F	ATTTCCCACCATTGCGGCTC
	xssK-8R	CAAGGGACATCCTGTTGGGC
	xssM-7F	GCCATGTTCGTGCTGGGTTC
	xssM-8R	GCCCAGAACCAAATACTGCGG
	xssN-8F	GCAAAGTCGGGTTGGAGTGG
	xssN-9R	CCAAGGCAAAGAACGGTAGGC
	xssP-8F	CGGCTTAACCGGAGAATGGC
	xssP-9R	CCCAAGCTCCAGCGTTTCTG
EMSA	xssEup-1F	AGGAAAGAAGTGTTCATGGG
	xssEup-2R	ATCTTTAAAGCCCCAGTCCC
	xssQ-5F28a	TATTTTCAGAGCCATATGGCAAAACGTTCCCTTA
	xssQ-6R28a	CTCGAATTCGGATCCTTAGCTAACCTTTTCGCC
	pET28a-1R	CATATGGCTCTGAAAATACAG
	pET28a-2F	GGATCCGAATTCGAGCTC

458

459 **Table S6.** List of mutants.

Strain name	Design
Δ*slr1943*	Complete deletion by Sp^R
Δ*slr1063*	Complete deletion by Sp^R
Δ*sll0501*	Complete deletion by Sp^R
Δ*slr1118*	Complete deletion by Sp^R
Δ*slr5054*	Partial deletion by Sp^R (= Δ xssK~M)
Δ*xssA*	Replacement of the the start codon by Sp^R and stop codon
Δ*xssB*	Replacement of the the start codon by Sp^R and stop codon
Δ*xssC*	Replacement of the the start codon by Sp^R and stop codon
Δ*xssE*	Replacement of the the start codon by Sp^R and stop codon
Δ*xssF*	Replacement of the the start codon by Sp^R and stop codon
Δ*xssG*	Replacement of the the start codon by Sp^R and stop codon
Δ*xssH*	Replacement of the the start codon by Sp^R and stop codon
Δ*xssI*	Replacement of the the start codon by Sp^R and stop codon
Δ*xssJ*	Replacement of the the start codon by Sp^R and stop codon
Δ*xssK*	Replacement of the the start codon by Sp^R and stop codon
Δ*xssM*	Replacement of the the start codon by Sp^R and stop codon
Δ*xssN*	Replacement of the the start codon by Sp^R and stop codon
Δ*xssO*	Replacement of the the start codon by Sp^R and stop codon
Δ*xssP*	Replacement of the the start codon by Sp^R and stop codon
Δ*xssQ*	Replacement of the the start codon by Sp^R and stop codon
Δ*xssR* *	Partial deletion by Sp^R
Δ*xssS* *	Partial deletion by Sp^R
Δ*xssR-S* *	Partial deletion by Sp^R
Δ*xssK~M* + Δ*xssS* *	*xssK~M*::Sp^R + *xssS*::Cm^R
OX-*xssR* #	slr0846_platform-Km^R-P_{trc}-XssS-T_{rrnB}
OX-*xssQ* #	IS203_platform-Cm^R-P_{trc}-XssQ-T_{rrnB}
Δ*xssQ* + OX-*xssR*	Simple combination
Δ*xssR* * + OX-*xssQ* #	Simple combination
OX-*xssP* #	Replacement of the the native promoter to Cm^R-P_{trc}
Δ*xssT*	Complete deletion by Km^R

460

461 *Almost complete segregation. #Partial segregation.

462

463 the transformed DNA in the multicopy genome was confirmed by PCR using primers listed in Table S5,

464 and the transformants are listed in Table S6.

465

466 ***Bloom formation***

467 The bloom was reproducibly formed using the two-step culture regime we developed in this

468 work. Before the bloom formation experiment, cells were precultured once in liquid after transfer from

469 plates. In the first step, cells inoculated at OD_{730} = 0.2 were grown with vigorous aeration under

470 continuous light at 31°C or 20°C for 48 h. Typically the cell density reached OD_{730} ~2. In the second

471 step, the culture was shifted to the standing condition without bubbling under the same continuous light

472 for another 48 h (or longer) for cells to rise to the surface. Regarding the mutants of transmembrane

473 glycosyltransferases, bloom formation was examined after 168 h of the second-step culture. The final

474 concentration of the photosynthesis inhibitor DCMU (3-(3,4-dichlorophenyl)-1,1-dimethylurea) was

475 100 μM.

476

477 ***EPS fractionation***

478 The fractionation method to isolate the crude EPS is shown in Fig. S1A. The viscous
479 materials including cells after the second step of culture were collected by filtration using a 1.0-μm pore
480 PTFE membrane (Millipore). The trapped materials were gently and carefully recovered from the
481 membrane using MilliQ water with the aid of flat-tip tweezers. The collected sample was vortexed and
482 then centrifuged at 20,000 × *g* for 10 min to remove cells. The supernatant constituted the crude EPS
483 that contained viscous EPS and possibly CPS.

484 The refined fractionation method to isolate EPS is shown in Fig. 1F. The entire culture at the
485 end of the first step, which did not contain gas bubbles, was first centrifuged at 10,000 × *g* for 10 min
486 to remove cells and CPS and then filtered through a 1.0-μm pore PTFE membrane. The trapped EPS
487 was carefully recovered as described above. The flowthrough of the filtration was regarded as free
488 polysaccharides, which were recovered by ethanol precipitation. CPS was released from the cell pellet

by vigorous vortexing with MilliQ water and recovered by centrifugation to remove cells (20,000 × *g* for 10 min).

Sugar quantification

Total sugar was quantified using the phenol-sulfate method (*DuBois et al., 1956*). A 100-µL aliquot of 5% (w/w) phenol was added to 100 µL of a sample in a glass tube and vortexed three times for 10 s. Then, 500 µL of concentrated sulfuric acid was added, and the tube was immediately vortexed three times for 10 s and then kept at 30°C for 30 min in a water bath. Sugar content was measured by absorption at 487 nm using a UV-2600PC spectrophotometer (Shimadzu, Japan, Tokyo). Any contamination of the BG11 medium was evident by slight background coloration. This background was subtracted on the basis of the extrapolation of absorption at 430 nm, where the coloration due to sugars was minimal. Glucose was used as the standard. Some EPS samples were highly viscous, so we vortexed and sonicated them before measurement. Statistical significance was determined using Welch's *t* test.

502

503 ***Sugar composition analysis***

504 The collected EPS samples were dialyzed with MilliQ water and then freeze-dried for 3 days.

505 Sugar composition was analysed by Toray Research Center, Inc. (Tokyo, Japan). A part of the fluffy

506 sample (WT, 0.298 mg; Δ*xssS*, 0.203 mg) was dissolved in 200 μL of 2 M trifluoroacetic acid and

507 hydrolysed at 100°C for 6 h. The treated sample was vacuum-dried with a centrifugal evaporator,

508 redissolved in 400 μL MilliQ water, and filtered through a 0.22-μm pore filter. This sample was used for

509 the analysis.

510 Monosaccharide composition was determined by HPLC with the LC-20A system (Shimadzu).

511 For neutral sugars, the column was TSK-gel Sugar AXG (TOSOH, Japan) and the temperature was 70°C.

512 The mobile phase was 0.5 M potassium borate (pH 8.7) at 0.4 mL/min. Post-column labelling was

513 performed using 1% (w/v) arginine and 3% (w/v) boric acid at 0.5 mL/min, 150°C. For uronic acids, the

514 column was a Shimpack ISA-07 (Shimadzu) and the temperature was 70°C. The mobile phase was 1.0

515 M potassium borate (pH 8.7) at 0.8 mL/min. Post-column labelling was performed using 1% (w/v)

516 arginine and 3% (w/v) boric acid at 0.8 mL/min, 150°C. The detector was a RF-10A_{XL} (Shimadzu), with

517 excitation at 320 nm and emission at 430 nm. The standard curves were prepared for each

518 monosaccharide with standard samples.

519 The SO_4^{2-} content was determined by anion exchange column chromatography using the

520 ISC-2100 system (Thermo Fisher Scientific, USA, Massachusetts). The column was eluted via a

521 gradient of 0–1.0 M KOH. The separation column was IonPac ASI l-HC-4 μm (Thermo Fisher

522 Scientific). Electric conductivity was used for detection.

523

524 ***Alcian blue staining***

525 The polysaccharides were stained with 1% Alcian blue 8GX (Merck) for 10 min in 3 % acetic

526 acid (pH 2.5) or 0.5 N HCl (pH 0.5) as previously described (*Di Pippo et al., 2013*).

527

528 ***qPCR***

529 The qPCR was performed as described in our previous work (*Maeda et al., 2018*). Cells were
530 harvested by centrifugation at 5000 × *g* for 10 min at 4°C. Cell disruption and RNA extraction were
531 done using an RNeasy Mini kit for bacteria (Qiagen, Venlo, Netherlands). In addition, cells were
532 disrupted five times by mechanical homogenization with zirconia beads (0.1-mm diameter) in a
533 microhomogenizing system (Micro Smash MS-100, TOMY SEIKO, Tokyo, Japan) at 5,000 rpm for 40
534 s. For cDNA preparation, RNA was reverse-transcribed using random primers (PrimeScript RT reagent
535 kit with gDNA eraser, Takara). Real-time PCR was performed using the THUNDERBIRD SYBR qPCR
536 Mix (Toyobo) and the Thermal Cycler Dice Real Time System II (Takara). The transcript level in each
537 strain was normalized to the internal control (*rnpB*). The primers used are listed in Table S5.

538

539 ***EMSA*** **(**electrophoretic mobility shift assay)

540 The expression and purification of recombinant His-tagged proteins and EMSA were

541 performed as described in our previous works (*Hirose et al., 2010, Maeda et al., 2014*). In brief, His-
542 tagged XssQ was expressed using pET28a vector system and *E. coli* C41(DE3) strain. The protein was
543 purified by Histrap HP column (Cytiva, Tokyo, Japan) and AKTA prime system (Cytiva). For probe and
544 native competitor, the upstream region of *xssE* was amplified with the primer set xssEup-1F/2R (total
545 251 bp). As a mutant competitor, the same region of the chemically synthesized DNA fragment
546 containing mutations in the two consensus sequences was used for amplification with the same primer
547 set as mention above. Labelling of the DNA probe, electrophoresis, and autoradiography were
548 performed as described (*Midorikawa et al., 2009*). We incubated the aliquots of the XssQ protein (0,
549 500, 1000, or 3000 ng/lane) with the radiolabeled probe for 30 min at room temperature. For competition,
550 3000 ng of XssQ was incubated with the probe and 20 pmol of unlabeled competitors (native or mutant).
551
552 ***RNA-seq analysis***
553 RNA-seq analysis was performed as described in our previous work (*Ohbayashi et al., 2016*).

554 Total RNA of *Synechocystis* 6803 was extracted as described in the qPCR protocol. The contaminated

555 genome DNA was removed by TURBO DNA-free™ Kit (Thermo Fisher Scientific).

556

557 ***Bioinformatics analysis***

558 The sequences of the proteins were obtained from NCBI (http://www.ncbi.nlm.nih.gov/) and

559 Pfam (http://pfam.xfam.org/) (*Finn et al., 2016*). The domain architecture was searched using the Simple

560 Modular Architecture Research Tool, SMART (*Letunic et al., 2015*). Glycosyltransferase classifications

561 were based on the CAZy database (http://www.cazy.org/) (*Henrissat, 1991, Lombard et al., 2013*).

562 Amino acid sequence similarity was evaluated by NCBI BLAST search.

563

564 **Acknowledgements**

565 This study was supported by Grants-in-Aid for JSPS Fellows 15J07605 and 19J01251 (to

566 K.M.), the Japan Society for the Promotion of Science for Scientific Research (16H06558 to M.I.), and

567 the JST for CREST program (JPMJCR1653 to M.I.).

568

569 **References**

570 Beard SJ, Hayes PK, Pfeifer F, Walsby AE. 2002. The sequence of the major gas vesicle protein,
571 GvpA, influences the width and strength of halobacterial gas vesicles. *FEMS microbiology*
572 *letters* **213**:149-157

573 Bellezza S, Albertano P, de Philippis R, Paradossi G. 2006. Exopolysaccharides of two
574 cyanobacterial strains from Roman hypogea. *Geomicrobiology Journal* **23**:301-310

575 Casero MC, Velázquez D, Medina-Cobo M, Quesada A, Cirés S. 2019. Unmasking the identity of
576 toxigenic cyanobacteria driving a multi-toxin bloom by high-throughput sequencing of
577 cyanotoxins genes and 16S rRNA metabarcoding. *Science of The Total Environment*
578 **665**:367-378

579 Chen M, Tian L-L, Ren C-Y, Xu C-Y, Wang Y-Y, Li L. 2019. Extracellular polysaccharide synthesis
580 in a bloom-forming strain of Microcystis aeruginosa: implications for colonization and
581 buoyancy. *Scientific reports* **9**:1-11

582 Chin T, Okuda Y, Ikeuchi M. 2018. Sorbitol production and optimization of photosynthetic supply
583 in the cyanobacterium *Synechocystis* PCC 6803. *Journal of biotechnology* **276**:25-33

584 Danot O, Marquenet E, Vidal-Ingigliardi D, Richet E. 2009. Wheel of Life, Wheel of Death: A
585 Mechanistic Insight into Signaling by STAND Proteins. *Structure* **17**:172-182. DOI:
586 10.1016/j.str.2009.01.001

587 De Philippis R, Vincenzini M. 1998. Exocellular polysaccharides from cyanobacteria and their
588 possible applications. *FEMS Microbiology Reviews* **22**:151-175

589 Dervaux J, Mejean A, Brunet P. 2015. Irreversible collective migration of cyanobacteria in eutrophic
590 conditions. *PLoS One* **10**:e0120906

591 Di Pippo F, Ellwood NT, Gismondi A, Bruno L, Rossi F, Magni P, De Philippis R. 2013.
592 Characterization of exopolysaccharides produced by seven biofilm-forming cyanobacterial
593 strains for biotechnological applications. *Journal of Applied Phycology* **25**:1697-1708

du Plooy S, Perissinotto R, Smit A, Muir D. 2015. Role of salinity, nitrogen fixation and nutrient assimilation in prolonged bloom persistence of *Cyanothece* sp. in Lake St Lucia, South Africa. *Aquatic Microbial Ecology* **74**:73-83

DuBois M, Gilles KA, Hamilton JK, Rebers Pt, Smith F. 1956. Colorimetric method for determination of sugars and related substances. *Analytical chemistry* **28**:350-356

Enomoto G, Narikawa R, Ikeuchi M. 2015. Three cyanobacteriochromes work together to form a light color-sensitive input system for c-di-GMP signaling of cell aggregation. *Proceedings of the National Academy of Sciences* **112**:8082-8087

Finn RD, Coggill P, Eberhardt RY, Eddy SR, Mistry J, Mitchell AL, Potter SC, Punta M, Qureshi M, Sangrador-Vegas A. 2016. The Pfam protein families database: towards a more sustainable future. *Nucleic acids research* **44**:D279-D285

Fisher ML, Allen R, Luo Y, Curtiss R, 3rd. 2013. Export of extracellular polysaccharides modulates adherence of the Cyanobacterium *synechocystis*. *PLoS One* **8**:e74514. DOI: 10.1371/journal.pone.0074514, PMID: PMC3769361

Flombaum P, Gallegos JL, Gordillo RA, Rincón J, Zabala LL, Jiao N, Karl DM, Li WK, Lomas MW, Veneziano D. 2013. Present and future global distributions of the marine Cyanobacteria Prochlorococcus and Synechococcus. *Proceedings of the National Academy of Sciences* **110**:9824-9829

Flores C, Lima RT, Adessi A, Sousa A, Pereira SB, Granja PL, De Philippis R, Soares P, Tamagnini P. 2019a. Characterization and antitumor activity of the extracellular carbohydrate polymer from the cyanobacterium Synechocystis DeltasigF mutant. *Int J Biol Macromol* **136**:1219-1227. DOI: 10.1016/j.ijbiomac.2019.06.152

Flores C, Santos M, Pereira SB, Mota R, Rossi F, De Philippis R, Couto N, Karunakaran E, Wright PC, Oliveira P, Tamagnini P. 2019b. The alternative sigma factor SigF is a key player in the control of secretion mechanisms in Synechocystis sp. PCC 6803. *Environ Microbiol* **21**:343-359. DOI: 10.1111/1462-2920.14465

620 Foster JS, Havemann SA, Singh AK, Sherman LA. 2009. Role of mrgA in peroxide and light stress
621 in the cyanobacterium Synechocystis sp. PCC 6803. *FEMS Microbiol Lett* **293**:298-304.
622 DOI: 10.1111/j.1574-6968.2009.01548.x
623 Freitas F, Alves V, Reis M. 2014. Bacterial polysaccharides: production and applications in cosmetic
624 industry Springer International Publishing Cham.
625 Fujishiro T, Ogawa T, Matsuoka M, Nagahama K, Takeshima Y, Hagiwara H. 2004. Establishment
626 of a pure culture of the hitherto uncultured unicellular cyanobacterium *Aphanothece*
627 *sacrum*, and phylogenetic position of the organism. *Applied and environmental*
628 *microbiology* **70**:3338-3345. DOI: 10.1128/AEM.70.6.3338-3345.2004, PMID: PMC427778
629 Ghosh T, Chattopadhyay K, Marschall M, Karmakar P, Mandal P, Ray B. 2009. Focus on antivirally
630 active sulfated polysaccharides: from structure-activity analysis to clinical evaluation.
631 *Glycobiology* **19**:2-15. DOI: 10.1093/glycob/cwn092
632 Harke MJ, Steffen MM, Gobler CJ, Otten TG, Wilhelm SW, Wood SA, Paerl HW. 2016. A review of
633 the global ecology, genomics, and biogeography of the toxic cyanobacterium, *Microcystis spp.*
634 *Harmful Algae* **54**:4-20
635 Hayashi T, Hayashi K, Maeda M, Kojima I. 1996. Calcium spirulan, an inhibitor of enveloped virus
636 replication, from a blue-green alga *Spirulina platensis*. *Journal of natural products* **59**:83-
637 87
638 Henrissat B. 1991. A classification of glycosyl hydrolases based on amino acid sequence similarities.
639 *Biochemical Journal* **280**:309-316
640 Hirose Y, Narikawa R, Katayama M, Ikeuchi M. 2010. Cyanobacteriochrome CcaS regulates
641 phycoerythrin accumulation in Nostoc punctiforme, a group II chromatic adapter.
642 *Proceedings of the National Academy of Sciences* **107**:8854-8859
643 Huisman J, Codd GA, Paerl HW, Ibelings BW, Verspagen JM, Visser PM. 2018. Cyanobacterial
644 blooms. *Nature Reviews Microbiology* **16**:471-483
645 Islam ST, Lam JS. 2014. Synthesis of bacterial polysaccharides via the Wzx/Wzy-dependent

646 pathway. *Canadian journal of microbiology* **60**:697-716

647 Jiao G, Yu G, Zhang J, Ewart HS. 2011. Chemical structures and bioactivities of sulfated
648 polysaccharides from marine algae. *Marine Drugs* **9**:196-223. DOI: 10.3390/md9020196,
649 PMID: PMC3093253

650 Jittawuttipoka T, Planchon M, Spalla O, Benzerara K, Guyot F, Cassier-Chauvat C, Chauvat F.
651 2013. Multidisciplinary evidences that *Synechocystis* PCC6803 exopolysaccharides operate
652 in cell sedimentation and protection against salt and metal stresses. *PLoS One* **8**:e55564

653 Karamanos NK, Piperigkou Z, Theocharis AD, Watanabe H, Franchi M, Baud S, Brezillon S, Go¨
654 tte M, Passi A, Vigetti D. 2018. Proteoglycan chemical diversity drives multifunctional cell
655 regulation and therapeutics. *Chemical reviews* **118**:9152-9232

656 Katzen F, Ferreiro DU, Oddo CG, Ielmini MV, Becker A, Pühler A, Ielpi L. 1998. Xanthomonas
657 campestris pv. campestrisgum Mutants: Effects on Xanthan Biosynthesis and Plant
658 Virulence. *Journal of bacteriology* **180**:1607-1617

659 Kawano Y, Saotome T, Ochiai Y, Katayama M, Narikawa R, Ikeuchi M. 2011. Cellulose
660 accumulation and a cellulose synthase gene are responsible for cell aggregation in the
661 cyanobacterium Thermosynechococcus vulcanus RKN. *Plant and Cell Physiology* **52**:957-
662 966

663 Kopf M, Klähn S, Pade N, Weingärtner C, Hagemann M, Voß B, Hess WR. 2014a. Comparative
664 genome analysis of the closely related Synechocystis strains PCC 6714 and PCC 6803. *DNA*
665 *research* **21**:255-266

666 Kopf M, Klähn S, Scholz I, Matthiessen JK, Hess WR, Voß B. 2014b. Comparative analysis of the
667 primary transcriptome of *Synechocystis* sp. PCC 6803. *DNA research* **21**:527-539

668 Kumar D, Kastanek P, Adhikary SP. 2018. Exopolysaccharides from cyanobacteria and microalgae
669 and their commercial application. *Current Science* **115**:234-241

670 Lapasin R, Pricl S, 1995. Industrial applications of polysaccharides *Rheology of Industrial*
671 *Polysaccharides: Theory and Applications.* Springer. p134-161.

672 Letunic I, Doerks T, Bork P. 2015. SMART: recent updates, new developments and status in 2015.
673 *Nucleic acids research* **43**:D257-D260
674 Lombard V, Golaconda Ramulu H, Drula E, Coutinho PM, Henrissat B. 2013. The carbohydrate-
675 active enzymes database (CAZy) in 2013. *Nucleic acids research* **42**:D490-D495
676 Maeda K, Narikawa R, Ikeuchi M. 2014. CugP is a novel ubiquitous non-GalU-type bacterial UDP-
677 glucose pyrophosphorylase found in cyanobacteria. *Journal of bacteriology* **196**:2348-2354
678 Maeda K, Tamura J, Okuda Y, Narikawa R, Midorikawa T, Ikeuchi M. 2018. Genetic identification
679 of factors for extracellular cellulose accumulation in the thermophilic cyanobacterium
680 *Thermosynechococcus vulcanus*: proposal of a novel tripartite secretion system. *Molecular*
681 *Microbiology* **109**:121-134
682 Mangan NM, Flamholz A, Hood RD, Milo R, Savage DF. 2016. pH determines the energetic
683 efficiency of the cyanobacterial CO2 concentrating mechanism. *Proceedings of the National*
684 *Academy of Sciences* **113**:E5354-E5362
685 Merel S, Walker D, Chicana R, Snyder S, Baurès E, Thomas O. 2013. State of knowledge and
686 concerns on cyanobacterial blooms and cyanotoxins. *Environment international* **59**:303-327
687 Midorikawa T, Matsumoto K, Narikawa R, Ikeuchi M. 2009. An Rrf2-type transcriptional regulator
688 is required for expression of psaAB genes in the cyanobacterium Synechocystis sp. PCC
689 6803. *Plant physiology* **151**:882-892
690 Mota R, Vidal R, Pandeirada C, Flores C, Adessi A, De Philippis R, Nunes C, Coimbra MA,
691 Tamagnini P. 2020. Cyanoflan: A cyanobacterial sulfated carbohydrate polymer with
692 emulsifying properties. *Carbohydrate Polymers* **229**:115525. DOI:
693 10.1016/j.carbpol.2019.115525
694 Mougous JD, Green RE, Williams SJ, Brenner SE, Bertozzi CR. 2002. Sulfotransferases and
695 sulfatases in mycobacteria. *Chemistry & biology* **9**:767-776
696 Mouhim RF, Cornet J-F, Fontane T, Fournet B, Dubertret G. 1993. Production, isolation and
697 preliminary characterization of the exopolysaccharide of the cyanobacterium *Spirulina*

platensis. *Biotechnology letters* **15**:567-572

Ngatu NR, Okajima MK, Yokogawa M, Hirota R, Eitoku M, Muzembo BA, Dumavibhat N, Takaishi M, Sano S, Kaneko T. 2012. Anti-inflammatory effects of sacran, a novel polysaccharide from Aphanothece sacrum, on 2, 4, 6-trinitrochlorobenzene–induced allergic dermatitis in vivo. *Annals of Allergy, Asthma & Immunology* **108**:117-122. e112

Ohbayashi R, Watanabe S, Ehira S, Kanesaki Y, Chibazakura T, Yoshikawa H. 2016. Diversification of DnaA dependency for DNA replication in cyanobacterial evolution. *The ISME journal* **10**:1113-1121

Okajima MK, Bamba T, Kaneso Y, Hirata K, Fukusaki E, Kajiyama Si, Kaneko T. 2008. Supergiant ampholytic sugar chains with imbalanced charge ratio form saline ultra-absorbent hydrogels. *Macromolecules* **41**:4061-4064

Panoff J-M, Priem B, Morvan H, Joset F. 1988. Sulphated exopolysaccharides produced by two unicellular strains of cyanobacteria, Synechocystis PCC 6803 and 6714. *Archives of microbiology* **150**:558-563

Pereira S, Zille A, Micheletti E, Moradas-Ferreira P, De Philippis R, Tamagnini P. 2009. Complexity of cyanobacterial exopolysaccharides: composition, structures, inducing factors and putative genes involved in their biosynthesis and assembly. *FEMS Microbiology Reviews* **33**:917-941

Pereira SB, Mota R, Vieira CP, Vieira J, Tamagnini P. 2015. Phylum-wide analysis of genes/proteins related to the last steps of assembly and export of extracellular polymeric substances (EPS) in cyanobacteria. *Scientific reports* **5**

Pereira SB, Santos M, Leite JP, Flores C, Eisfeld C, Büttel Z, Mota R, Rossi F, De Philippis R, Gales L. 2019. The role of the tyrosine kinase Wzc (Sll0923) and the phosphatase Wzb (Slr0328) in the production of extracellular polymeric substances (EPS) by *Synechocystis* PCC 6803. *MicrobiologyOpen* **8**:e00753

Sasisekharan R, Raman R, Prabhakar V. 2006. Glycomics approach to structure-function

relationships of glycosaminoglycans. *Annu Rev Biomed Eng* **8**:181-231

Schmid J, Sieber V, Rehm B. 2015. Bacterial exopolysaccharides: biosynthesis pathways and engineering strategies. *Frontiers in microbiology* **6**:496. DOI: 10.3389/fmicb.2015.00496, PMID: PMC4443731

Stanier R, Kunisawa R, Mandel M, Cohen-Bazire G. 1971. Purification and properties of unicellular blue-green algae (order *Chroococcales*). *Bacteriological reviews* **35**:171-205

Steffen MM, Li Z, Effler TC, Hauser LJ, Boyer GL, Wilhelm SW. 2012. Comparative metagenomics of toxic freshwater cyanobacteria bloom communities on two continents. *PLoS One* **7**:e44002

Vial L, Hommais F. 2020. Plasmid - chromosome cross - talks. *Environmental Microbiology* **22**:540-556

Walsby A. 1994. Gas vesicles. *Microbiological reviews* **58**:94-144

Wardrop D, Keeling D. 2008. The story of the discovery of heparin and warfarin. *British journal of haematology* **141**:757-763

Wei K, Jung S, Amano Y, Machida M. 2019. Control of the buoyancy of Microcystis aeruginosa via colony formation induced by regulating extracellular polysaccharides and cationic ions. *SN Applied Sciences* **1**:1573

Willis LM, Whitfield C. 2013. Structure, biosynthesis, and function of bacterial capsular polysaccharides synthesized by ABC transporter-dependent pathways. *Carbohydrate Research* **378**:35-44

Woodward L, Naismith JH. 2016. Bacterial polysaccharide synthesis and export. *Current Opinion in Structural Biology* **40**:81-88

Yoshihara S, Suzuki F, Fujita H, Geng XX, Ikeuchi M. 2000. Novel putative photoreceptor and regulatory genes required for the positive phototactic movement of the unicellular motile cyanobacterium *Synechocystis* sp. PCC 6803. *Plant and Cell Physiology* **41**:1299-1304